

**Review**

## **Surface modification of carbon nanotubes and their nanocomposites for fuel cell applications: A review**

**Okechukwu Okafor<sup>1,\*</sup>, Abimbola Popoola<sup>1</sup>, Olawale Popoola<sup>2</sup> and Samson Adeosun<sup>3</sup>**

<sup>1</sup> Chemical, Metallurgical & Materials Engineering, Tshwane University of Technology, P.M.B X680, Pretoria, South Africa

<sup>2</sup> Electrical Engineering, Tshwane University of Technology, P.M.B X680, Pretoria, South Africa

<sup>3</sup> Affiliation Metallurgical and Materials Engineering, University of Lagos, Yaba, Lagos, 23401, Nigeria

**\* Correspondence:** Email: 222892236@tut4life.ac.za; Tel: +27-73-404-4314.

**Abstract:** Carbon nanotubes (CNTs) have drawn great attention as potential materials for energy conversion and storage systems such as batteries, supercapacitors, and fuel cells. Among these energy conversion and storage systems, the fuel cells had stood out owing to their high-power density, energy conversion efficiency and zero greenhouse gasses emission. In fuel cells, CNTs have been widely studied as catalyst support, bipolar plates and electrode material due to their outstanding mechanical strength, chemical stability, electrical and thermal conductivity, and high specific surface area. The use of CNT has been shown to enhance the electrocatalytic performance of the catalyst, corrosion resistivity, improve the transmission performance of the fuel cell and reduce the cost of fuel cells. The use of CNTs in fuel cells has drastically reduced the use of noble metals. However, the major drawback to the utilization of pristine CNTs in fuel cells are; poor dispersion, agglomeration, and insolubility of CNTs in most solvents. Surface engineering of CNTs and CNT nanocomposites has proven to remarkably remedy these challenges and significantly enhanced the electrochemical performance of fuel cells. This review discusses the different methods of surface modification of CNTs and their nanocomposite utilized in fuel cell applications. The effect of CNTs in improving the performance of fuel cell catalyst, membrane electrode assembly and bipolar plates of fuel cells. The interaction between the CNTs catalyst support and the catalyst is also reviewed. Lastly, the authors outlined the challenges and recommendations for future study of surface functionalized CNTs composite for fuel cell application.

**Keywords:** carbon nanotubes; functionalization; fuel cells; electrocatalyst; nanocomposite

---

## 1. Introduction

The increase in the global energy demand and the environmental challenges associated with the use of fossil fuel, which has been the highest source of energy in the world. The world has been faced with high global warming, economic and political instability caused by fossil fuel depletion which has led to increased attention and exploration of renewable sustainable energy system [1]. Among sustainable energy systems, Fuel cell system has been considered as energy storage technology that can drastically tackle these issues. Fuel cell system has been considered as a good replacement for batteries, steam turbines and combustion engines. Fuel cells are widely employed in small- and large-scale power plant, back-up power source for buildings and in portable electronics [2].

The material selection in fuel cell design is critical and strongly determines the durability, electrochemical performance, and the efficiency of the fuel cell system [3]. A typical fuel cell is basically made up of two electrode (anode and cathode), fuel source and electrolyte.

The electrocatalyst is a key component of the water-splitting process, which is a significant energy storage system for the efficient production of hydrogen in fuel cells. Electrode materials for fuel cells are typically metal hydroxide-based electrode catalysts. However, they have several drawbacks that limit their ability to contribute to energy storage technologies, including high cost, poor accessibility, and short service lives [4].

CNTs have found great application in energy conversion and storage systems such as electrode materials for batteries, supercapacitors, and fuel cells. CNTs can be used to efficiently store hydrogen energy as it allows the flow of electrons and enhance the activity of catalyst. In a fuel cell system, CNTs have been added to carbon anode with metal catalyst to enhance the electrocatalytic reaction in the fuel cell. The major drawback in the full utilization of CNTs in energy system is their poor solubility in solvent (aqueous and organic solvent) caused by the strong Van der Waal bond between the carbon nanotubes. In addition to the poor dispersibility of CNTs, they have high surface inertness [5,6]. Studies have revealed many ways to solve these challenges such as surface modification of CNTs by introducing chemical moieties [7]. Functionalized CNT nanocomposite with polymer, noble metals and other compound have been explored by researchers as electrocatalyst support materials [5].

Hence, this review study tends to discuss different synthesis of CNTs, surface engineering of CNTs, CNT nanocomposite and their application in fuel cell systems. The concepts, and cyclic stability of fuel cells are also covered, along with challenges and prospects in the utilization of CNT composite in the construction of functional fuel cells.

## 2. Overview of carbon nanotube

CNTs are a nanostructured allotrope of carbon. It is a seamless rolled-up sheet of graphene in a tube. CNT has a two dimensional (2D) structure and a hexagonal lattice crystal structure with high aspect ratio [8]. It was first discovered in 1991 by Sumio Iijima [9]. CNTs have recently attracted great attention from researchers due to their unique electronic and electrical properties, high stability, and high surface area ( $700\text{--}1000\text{ m}^2\text{g}^{-1}$ ). CNTs find many applications in electronics, nanotechnology, optics, energy storage and transformation [10] due to their unique thermal conductivity, chemical

stability, mechanical properties, and electrical and electronic properties. The chemical characteristic of CNT strongly depends on the diameter of the nanotube. The smaller the diameter of CNT the higher the chemical reactivity due to the high curvature of the nanotube [11]. There are two basic types of CNT: single-wall carbon nanotube (SWCNT) and multiwall carbon nanotube (MWCNT) as shown in Figure 1. SWCNT is CNT with a single wall of diameter 1–2 nm. It has a mixture of metallic and semiconducting properties. This type of CNT mostly finds application in miniaturized electronic systems. MWCNTs are nanotubes with multiple rolled layers of graphene sheet with a diameter in the range of 2–100 nm [12]. The spacing between the walls of MWCNTs is approximately the spacing between two graphite planes (about 0.334 nm). The length, diameter structure and shape of CNTs strongly determine their characteristics [12]. CNTs can possess different structures such as Zigzag, chiral, and armchair nanotube structures based on the angle the graphene sheets can be rolled into tubes. These structures determine the electrical and electronic properties for instance zigzag and chiral CNTs can be either semiconducting or metallic, while armchair CNTs are metallic.

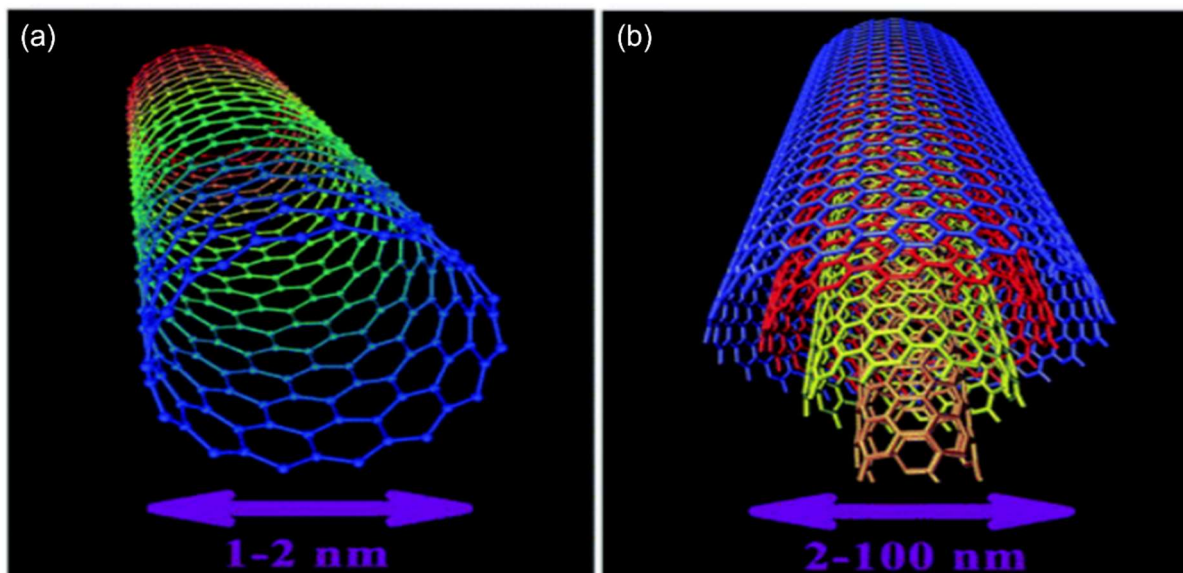


**Figure 1.** A schematic representation of (a) single wall carbon nanotube SWCNT and (b) multi wall carbon nanotube MWCNT [12].

### 2.1. Methods of synthesizing CNT

A lot of CNT synthesis methods have been reported in the literature, but three major techniques used for CNT preparation are arc discharge, chemical vapor deposition, and laser ablation. Other synthesis methods such as plasma, hydrothermal/sonochemical, microwave, solvothermal, liquid phase synthesis, plastic pyrolysis methods, and flame synthesis have also emerged [13,14]. However, these methods are complex to control and produce a very low yield of CNTs. The method of synthesis of CNT greatly determines the type of CNT produced, and it influences the properties and potential applications of CNT [15].

**Arc discharge method:** it is the first synthesis method used by Iijima in 1991 for CNT production. CNTs are produced in a vacuum chamber or inert atmosphere by applying direct current (dc) arc discharge between two graphite electrodes. The use of vacuum or inert (He or Ar) environment is to

prevent the oxidation of the carbon at elevated temperatures. The anode is made of graphite and a small amount of catalyst whereas the cathode is made of pure graphite. The synthesis takes place at temperatures between 2000 and 3000 °C. At this temperature carbon (graphite) evaporates from the anode and condenses at the cathode surface producing CNTs and soot [16]. These products are collected and purified to obtain only CNTs. The type, morphology, and properties of the CNTs produced using arc discharge method strongly depends on synthesizing parameters such as pressure of the inert gas, the stability of the dc arc, growth temperature, morphology of the graphite electrodes and catalyst type. The production of SWCNTs requires the use of a catalyst, and the SWCNTs grow and cluster between the anode and the cathode. Some of the catalysts used in arc discharge synthesis include Fe, Ni, Co, Ag, Fe-No, Co-Ni, Co-Cu, and Ni-Ti. In MWCNTs production catalyst is not required and MWCNTs growth takes place strictly on the cathode. This synthesis technique is highly efficient and produces CNTs with high crystallinity. However, Arc discharge synthesis produce low yield of CNTs accompanied with impurities such as fullerenes, amorphous carbon, carbon soot and particles from the metal catalyst used in the synthesis [17]. Another disadvantage of this method is that the CNTs are highly misaligned and contain a high presence of amorphous carbon. Additionally, this method is quite costly due to its high energy consumption and the requirement of a large quantity of graphite [17].

**Laser ablation method:** the laser ablation method is an eco-friendly, simple, and reliable method to produce high yield. It offers other advantages such as being inexpensive, providing high purity of the product, requiring no vacuum, and not needing a catalyst for production [18]. This method, graphite target is vaporized using pulse and laser energy at a temperature of about 1200 °C and subsequently followed by cooling and condensation of carbon onto a substrate to produce CNT. This method also utilizes catalysts to enhance the growth of the CNTs [19]. Studies had shown that the quality of the CNTs is optimum at the temperature of 1200 °C, below this temperature the structural quality of CNTs decreased with increased defect [20]. Also, the properties of the CNTs produced in the laser ablation method depend on the morphology of the carbon agglomerates, the interaction of catalyst with the graphite, and the laser parameters such as repetition rate, pulse width, laser fluence and wavelength [21]. CNTs grown through laser ablation method has very low metallic impurities [22]. The utilization of this method is limited by the high cost of the machinery, as well as by large particle agglomeration and aggregation, and high energy consumption [21,23].

**Chemical vapor deposition (CVD):** chemical vapor deposition has been widely used as a CNTs synthesizing method. It is used in depositing thin films of pure materials on a substrate. It involves the thermal decomposition of gaseous precursors in a reactor chamber at a certain applied pressure and temperature. Growing CNT using CVD involves the vaporization of carbon sources using thermal sources from either a resistive heated coil or plasma [24,25]. During this process, the substrate is prepared with a metal catalyst (e.g. Fe, Ni and Co) and then heated to a temperature between 600 to 700 °C. The carbon-containing gas decomposes at the surface of the catalyst and is thereafter transported to the edge of the substrate where CNTs are formed. Hydrocarbons such as acetylene, ethylene, xylene, methane, toluene, and methane are the most utilized carbon sources for this process. Some of the most used substrate include zeolite, alumina, Si, quartz, and silicon carbide [24,26]. The properties of CNT produced using CVD depend on the carbon source, reaction temperature and gas flow pressure. The CVD technique is majorly divided into two: thermal chemical vapor deposition (TCVD) and plasma enhanced chemical vapor deposition (PECVD) [26]. Low temperature TCVD is carried out by using reaction species that can decompose at low temperature. Study has shown that low temperature TCVD

produce short and tangled CNT and contain many structural defects [27]. PECVD makes use of plasma from sources like inductive coupled radio frequency, capacitive coupled radio frequency, and direct current. This method was introduced to address the challenges of high-temperature TCVD by utilizing plasma to facilitate the decomposition of the carbon source at significantly lower temperatures. It operates at low temperatures and can be used to grow well-aligned CNTs. Some advantages of CVD over other methods include the ability to control the reaction and direct the deposition of thin films onto the substrate to the desired region. Consequently, there is an improvement in controlling the properties of the CNTs, such as diameter, length, and chirality [26,28].

CVD produces well-aligned CNTs. Additionally, the CVD method allows carbon source materials to be inserted into the reactor chamber from an external reservoir without contaminating the growth of CNTs on the substrate. However, this process has several disadvantages: it involves the use of flammable and explosive liquids and gases, as well as high temperatures. Furthermore, the CVD process is associated with the production of metallic CNTs, which limits their utilization in flexible electronics [26,29,30]. Figure 2 shows the schematic representation of the three major techniques used in the production of CNTs.

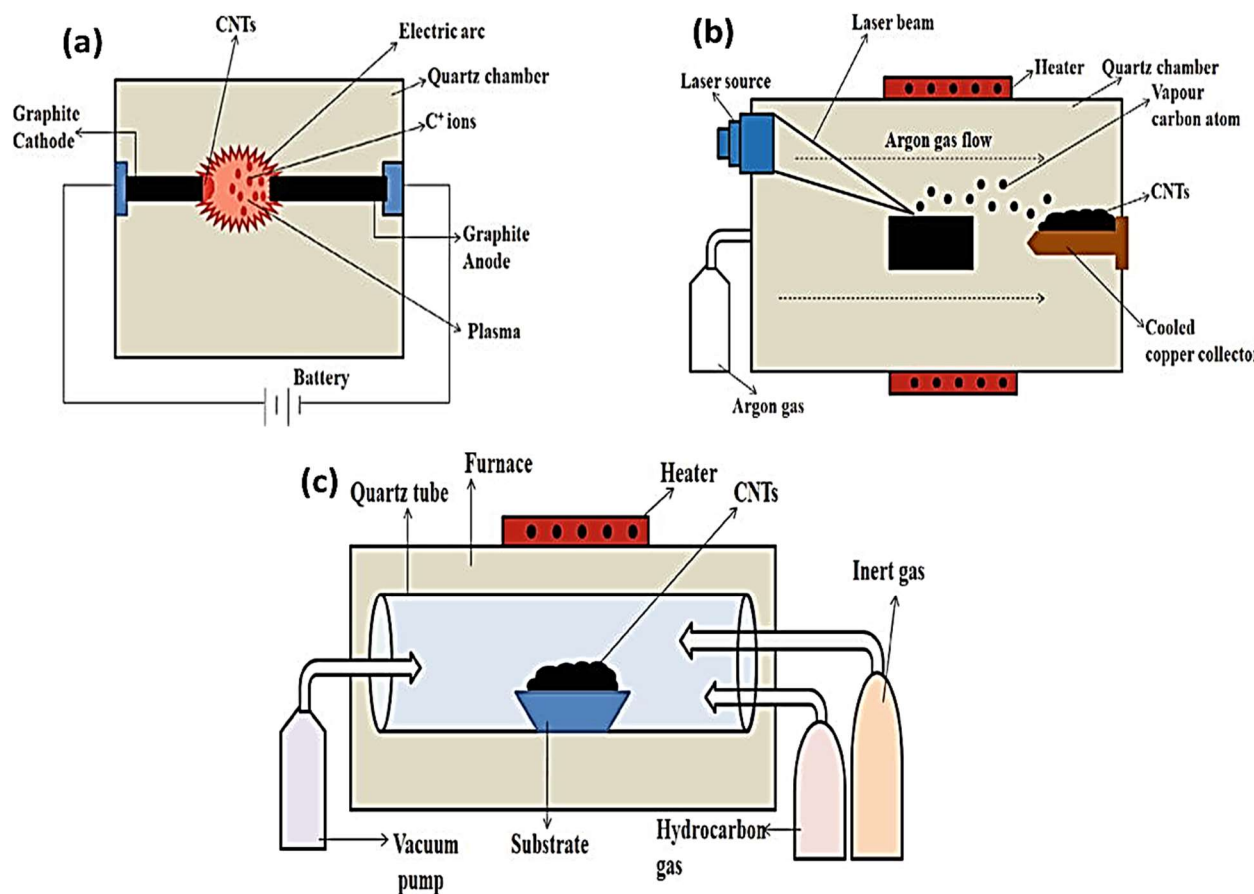


**Figure 2.** Diagrammatic representation of major CNT synthesis techniques: (a) arc discharge process, (b) laser abrasion and (c) chemical vapor deposition method [31].

## 2.2 Surface modification of CNTs

The major drawback in the full utilization of CNTs in energy systems is their poor solubility in solvent (aqueous and organic solvent) caused by the strong Van der Waal bond between the carbon nanotubes. In addition to the poor dispersibility of CNTs, they have high surface inertness [32]. Studies have revealed many ways to solve these challenges such as surface modification of CNTs by introducing chemical moieties [7]. Surface modification of CNTs mostly utilizes sidewall and open-end functionalization of CNTs. This functionalization strongly determines the dispersion, nanotube solubility and stress distribution and so is very important for the processability and potential application of the CNT composite. Surface functionalization is categorized into two groups: physical and chemical modification. Physical technique utilizes mechanical means such as crushing, milling, ultrasonication and friction to modify the surface chemistry of CNTs [32]. These physical techniques boost the internal energy and surface activity of CNTs, causing the tubes to interact with or attach to other substances to achieve the goal of surface modification. In these techniques, CNTs are dispersed using strong shear forces or ultrasonic processing [32,33]. Additionally, high-energy surface modification of CNTs using energy sources such as ultraviolet, plasma beam, electron beam, high-energy corona discharge, and  $\mu$ -ray has been employed as effective surface functionalization technique [33–35]. The chemical functionalization method is subdivided into two namely: covalent functionalization and non-covalent functionalization. Figure 3 shows the different classifications of CNTs functionalization.

### 2.2.1. Covalent functionalization of CNT

Covalent functionalization involves the covalent attachment of chemical moieties on the conjugate skeleton of the nanotubes. Covalent functionalization can be carried out on the sidewall of the nanotube or at the end caps which will produce different effects on the CNT [36]. The end caps of CNTs structure are the most reactive and mostly contain fullerene structure. Chemical functionalization mostly involves an oxidative treatment of the CNT with acid (mostly nitric acid and sulfuric acid). When the CNT undergoes oxidation, it yields oxygen-containing functional group such as hydroxyl ( $-\text{OH}$ ) and/or carboxylic acid ( $-\text{COOH}$ ) functional group at the sidewall and the ends of the nanotubes. These functional groups serve as chemical derivatization sites. For instance,  $-\text{COOH}$  groups allow the covalent coupling of molecules through the formation of ester and amide bonds [37]. Hence, research has shown the greater the cylindrical curvature of the nanotube sidewall the higher the chemical reactivity of the functionalized sidewall CNTs. The chemical reactivity of the CNTs also depends on the defects present on the ends and the sidewall of the CNTs. For instance, the stone-wale defect present on the sidewall of SWCNTs resulted in an increased chemical reactivity of the nanotube structure [38]. A lot of studies have been reported on the covalent functionalization of CNTs (SWCNT and MWCNT) over the past decades [39,40]. Goyanes et al. [41] functionalized MWCNTs with nitric acid and a mixture of nitric acid and sulfuric acid (at the ratio of 1:3 by volume) using ultrasonication treatment. The result obtained showed the formation of C–O functional groups on the surface of the CNTs at ultrasonication time of 2 h. However, at a longer ultrasonication time of 6 h, the regular structure of the nanotube is destroyed leading to shortening of the nanotube films. The concentration of functionalized group on the surface of SWCNT is in direct proportion with the reflux time. The open-end functionalization of SWCNTs using concentrated  $\text{HNO}_3$  revealed an effective functionalization in 4 h without compromising the characteristics and electronic nature of CNT. At functionalization

treatment above 4 h, the concentration of the  $-COOH$  functional group increased and this eventually damages the structure of CNT. Also, the CNTs begin to lose their electronic nature due to an increase in defects [7]. Malikov et al. [42] used two different strong oxidizing agents  $HNO_3$  and  $KMnO_4$  to functionalize MWCNTs and observed that  $KMnO_4$  has more oxidation potential than nitric acid. Sidewall functionalization of CNTs using halogen (Cl, F and Br) and hydrogen has been studied and reported to effectively increase the reactivity and dispersibility of CNTs in polar solvents [43–45]. Fluorination of CNTs increases the compressive strength, thermal conductivity properties and dispersibility of CNT in polymer solution [46]. Hydrogen functionalization of oxidized CNTs has been employed using gas phase surface modification technique to increase the active sites on CNTs and reduce unselective oxidation of the nanotube catalyst for oxygen dehydration process [44]. The chemical functionalization of CNTs makes it possible for them to be dispersed in a variety of polar solvents including water. Additionally, the covalent attachment of these functional groups reduces the Vander Waals interaction between the CNTs by altering the hydrogen bonding which encourages the disentangling of CNT bundles and reduces the stacking and layering of the CNTs [47]. Covalent functionalization converts the hydrophobic nature of CNT to become hydrophilic thereby improving phase adhesion of the nanotube with the matrix material. Chemical covalent functionalization can also be used to attach polymer material (epoxy, polyamide, polyhedral oligomeric silsesquioxane [48], and inorganic materials such as ceramics ( $TiO_2$ ,  $Fe_3O_4$  and  $TiCl_4$ ) on CNTs to form nanocomposite with enhance physical and chemical properties for numerous applications [49–51].

The drawbacks in covalent functionalization of CNTs are firstly, the damaging effect of the strong acid and ultrasonication process especially when done at a longer duration, which creates large defects on CNTs and destroys the regular graphene-type structure of the nanotube. It also involves the transition from  $sp^2$  hybridized state to  $sp^3$  hybridized state accompanied by loss of the p-conjugate system which is detrimental to the mechanical properties of the CNTs. It also results in disruption of  $\pi$  electrons which adversely affects the electronic and thermal conductivity of the CNTs. Secondly, covalent functionalization mostly involves the use of concentrated strong acids as oxidants which are very toxic to the environment [47].

### 2.2.2. Non-covalent functionalization

It involves the wrapping or supramolecular adsorption of different functional molecules onto CNTs. In noncovalent functionalization, CNTs can be wrapped with aromatic compounds, polymers, surfactants, or biomolecules [52]. The non-covalent functionalization of CNTs is achieved by  $\pi-\pi$  noncovalent interaction, between the  $\pi$  bond of the  $sp^2$  hybridized orbital of the carbon atom and the  $\pi$ -bond of the functional polymer, macromolecules, aromatic compound, or surfactants utilized as the activators. Supramolecular complexes are formed on the CNTs surfaces which will result in an improvement in the solubility and dispersion of the CNT in many conjugate polymers [53,54]. The non-covalent functionalization of CNTs is accomplished either through enthalpy-driven interactions, such as  $CH-\pi$ ,  $\pi-\pi$ , and  $NH-\pi$ , between the CNT surface and the dispersants, or through entropy-driven interactions, or hydrophobic interactions employing surfactants [47,52]. Some of the surfactants studied for the dispersion of CNTs include sodium dodecyl benzene sulfonate, sodium dodecyl sulphate, cetyltrimethylammonium bromide, and sodium cholate [55–58]. Non-covalent functionalization unlike the covalent functionalization does not affect the structural and electronic properties of the CNTs [59]. However, due to a potential weak force acting between the wrapping molecules and the nanotube

surface, the efficiency of the CNT load transfer capacity may be reduced. There are several non-covalent methods for nanotube functionalization, including polymer wrapping, surfactant-assisted dispersion, and the polymerization-filling method. Non-covalent functionalization of CNTs with polymers is an effective way to disperse the tubes in aqueous and non-aqueous solvents without damaging their unique structure and thus preserving their intrinsic properties. For instance, MWCNT functionalized with poly(3-hexylthiophenes) (P3HT) yielded a composite that can disperse in chloroform ( $\text{CHCl}_3$ ) solvent and possessed improved mechanical and electrical conductivity. P3HT-MWCNT composite (10 wt.% of MWCNT) prepared by ultrasonication method was found to be photochemically stable in not degrade easily upon exposure to ultraviolet light. It also showed increased conductivity when compared with pristine P3HT and MWCNTs [60]. A study of pyrene functionalized with P3HT wrapped SWCNT produced an SMCNT/pyrene-P3HT composite with  $\pi-\pi$  noncovalent interaction between the SWCNT and the pyrene which prevented the direct interaction between SWCNT and P3HT. The clusters of SWCNT in the composite were drastically reduced while the dimension increased than pristine SWCNT. The microstructural examination revealed a smooth film and well-dispersed SWCNTs in the composite [61]. In a similar study, poly (3-octyl-2,5-diyl thiophene) (P3OT) matrix reinforced with SWCNT using the alcoholic chemical vapor deposition (ACCVD) technique produced a composite with increased mechanical properties [62].

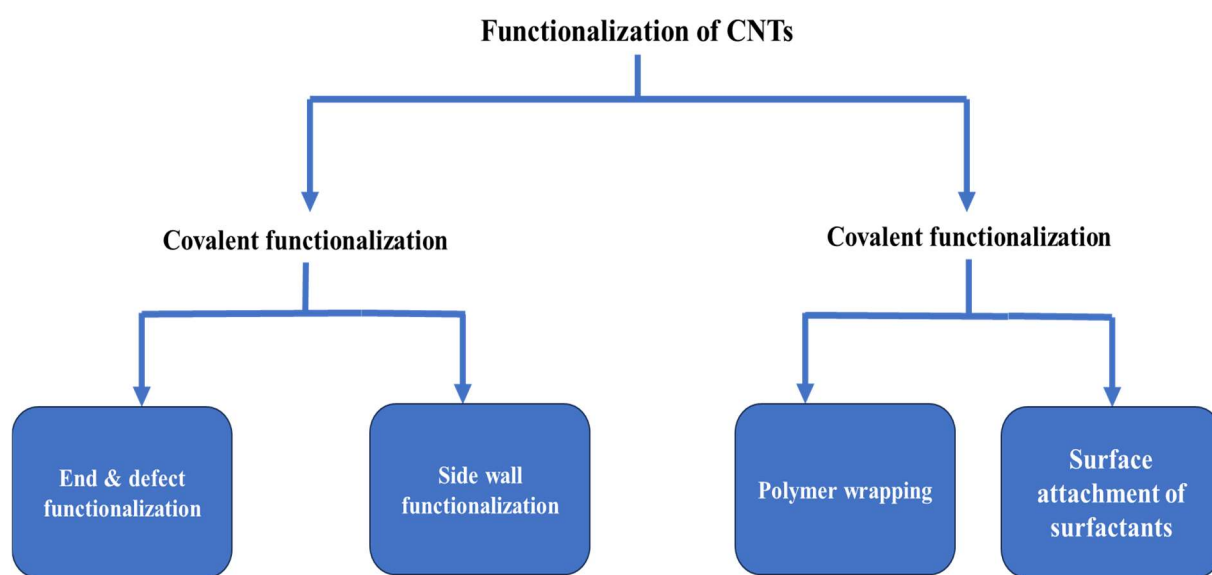


**Figure 3.** Diagrammatic representation of classification of CNT functionalization.

### 2.3. Functionalized CNT/polymer nanocomposite

The use of CNTs as a filler has been shown to increase the thermal conductivity and mechanical properties of the composite even at low concentrations of CNT [63]. Polymer/CNT composites have improved mechanical properties because of load transfer from a low elastic modulus polymer to a high modulus CNT filler. CNT has a high aspect ratio of about 106 and a high interfacial area ( $>1300 \text{ m}^2\text{g}^{-1}$ ) which favor reinforcement and electrical percolation at a low volume fraction [64]. Polymer/CNT composite has improved electrical conductivity, low thermal coefficient of expansion, elastic modulus, and stiffness at low concentrations of CNTs [63,65]. The incorporation of CNTs into polymer matrix

has been widely studied. There are diverse ways of incorporating CNT fillers into polymer composite to achieve fine dispersion of the fillers in the polymer matrix with drastically reduced agglomeration and entanglement. Some of the techniques explored for the synthesis of polymer/functionalized CNT include solution mixing, layer-by-layer assembly, melt processing and melt blending technique and in situ polymerization. Hong et al. [64] prepared functionalized MWCNT/epoxy composite via three roll milling process. The CNT was functionalized with carboxylic acid. Thereafter, uncured epoxy was premixed in various concentrations to create a CNT paste. The CNT pastes were then three-rolled for several minutes as the distance between the rolls gradually shrunk. Mixed CNT pastes were used for curing, and they were placed on a sample holder, heated for 24 h at 60 °C. Results show that the functional group was responsible for the effect on CNTs which enhance the isotropic bonding with the polymer and homogeneous dispersion of the nanotube in the epoxy matrix. The shear force exerted during the three-roll milling enhanced the thermal and mechanical properties of COOH-CNT/epoxy composite. Polymer/CNT composite synthesized by mechanical blending and solution casting showed high electrical conductivity and improved thermal and mechanical stability possibility of the composite. SWCNT/poly (ethylene succinate) synthesized by solvent casting and ultrasonication: the CNT was responsible for the enhanced crystallinity of the polymer composite [66]. Roy et al. [67] prepared HNO<sub>3</sub> functionalized SWCNT reinforced in polyvinylidene fluoride (PVDF) via ultrasonication. The ultrasonication enhanced the chemical interaction of the PVDF matrix and the acid functionalized SWCNTs. It also provides the energy required to transform the non-electroactive  $\alpha$ - phase of PVDF to the electroactive  $\gamma$ -polar phase. The presence of the C=O on the CNT filler surface resulted in the proper dispersion and interaction which promoted the  $\beta$  phase growth and subsequently resulted in the improvement in electrical, thermal, and mechanical properties of the composite. Ultrasonication time affects the crystallization of the composite. There was a strong interaction between the oxygen atom with  $\pi$  orbital in COOH-SWCNT and the hydrogen atom with positive charge PVDF which resulted in an increased mechanical and electrochemical property. Functionalization time plays a key role in the SWCNT structure. The author reported an optimum functionalization time of 4 h. When functionalization is carried out at quite a short duration, there is not enough time to attach the functional group to the polymer matrix. However, when the duration of functionalization is extended beyond the optimum time excessive damage is done to the nanotube structure thereby reducing the mechanical and other physical properties of the SWCNTs. In a certain study, it was reported that the reinforcement of high-density polyethylene (HDPE) matrix with 2 wt.% functionalized CNT resulted in a 35% increase in the elastic modulus of the HDPE/CNT nanocomposite due to the strong interfacial bonding between the polymer and the CNT. The enhanced mechanical properties of the HDPE/CNT composite were attributed to the uniform dispersion of CNT in the polymer matrix which result in the effective transfer of load from the CNT fillers to the polymer matrix [68]. Zadehnazari and Takassi [69] synthesized 3,5-diamino-N-(1,2,4)-(triazole-3-yl)-benzamide (DTB) functionalized MWCN/poly (benzimidazole-imide (PBI) composite and examined the thermal, mechanical, and morphological characteristics. The composite was synthesized via solvent evaporation technique. The composite was prepared with 1, 2 and 5 wt.% of DTB functionalized MWCNT. The amorphous and rigid structure of PBI was modified by the addition of functionalized MWCNT into a crystalline structure based on the formation of hydrogen bonds. DTB-MWCNT adhered strongly to PBI polymer matrix which increased the polarity caused by the functional group on the composite surface. There was an increase interaction between the surface of polymer matrix and the functional groups on the surface of the DTB-MWCNT filler. The DTB functionalization reduced the interspace between the MWCNTs and

modified the surface morphology of the MWCNTs increasing the aggregated structure due to the improved interaction between the functionalized MWCNTs. DTB acts as a crosslink for adjacent MWCNTs. DTB-MWCNT/PBI exhibit high thermal conductivity as the filler prevents the accumulation of heat at different points on the polymer backbone. Also, the thermal decomposition of the functionalized composite was drastically reduced compared to the pristine PBI. The increase in tensile strength and elastic modulus of DTB-MWCNT/PBI composite was due to the strong interaction between the PBI matrix and DTB-MWCNT and the introduction of hydrogen bonds and other secondary bonds. It was affirmed DTB-MWCNT was an effective reinforcing material as it effectively absorbed the load from the polymer. The improved solubility of the composite material in dimethylacetamide (DMA), dimethylformamide (DMF) and dimethyl sulfoxide (DMSO) was as result of the chemical interaction between the benzimidazole group, polar amide and triazole ring functional group with the polymer matrix backbone.

#### 2.4. Functionalized CNT/metal oxide (CNT/MO) nanocomposite

Metal oxides (MOs) have been actively studied due to their high strength and modulus of elasticity. However, their application is challenged by their low fracture toughness, brittleness, and poor intrinsic conductivity. Hence the development of CNT/MO nanocomposite by dispersing MOs particles on a CNTs conductive matrix which has a higher surface area to produce novel materials with unique functionalities in terms of mechanical, optical and electronic performance [70]. CNT/MO nanocomposite such as CNT/SnO<sub>2</sub>, CNT/Co<sub>3</sub>O<sub>4</sub>, CNT/Fe<sub>3</sub>O<sub>4</sub>, and CNT/Cr<sub>2</sub>O<sub>3</sub> has drawn the interest of researchers in energy storage and conversion system due to their long cyclability and rate capability [71,72]. Depending on the amount of CNT in relation to the ceramic oxide. CNT/MO can be grouped either as MO decorated on CNT or Mos reinforced with CNT. The preparation of CNT/MO nanocomposite mostly involve 3 stages which include: (i) surface functionalization of pristine CNT using strong oxidizing agent, (ii) decoration or deposition of metal nanoparticles on the CNT surface, and (iii) thermal treatment of the nanocomposite [73]. In CNT/MO nanocomposite, the metal oxide provides a large surface area for the adsorption of electrolyte while the CNT provides a conductive network for electron mobility and accommodation for volumetric changes that might occur during use as an electrode material [74]. In the study of CNT/MO composite, their two kinds of bonds are mostly considered which are metal–carbon (M–C) bond and metal–oxygen–carbon (M–O–C). Research have proved that the type of chemical bond and the interfacial bonding between the constituent material greatly affects the mobility or charges along the material and the overall electrochemical performance of the composite electrode material [75]. Cheng et al. [72] examined the effect of adjusting the interfacial bonding of CNTs/SnO<sub>2</sub> composite synthesized through hydrothermal technique on the electrochemical performance of the nanocomposite. The research outcome showed that the CNTs/SnO<sub>2</sub> composite with more Sn–C bonds has higher reversible capacity than the composite with more Sn–O–C bonds. This is due to the fast electron transfer path of CNTs/SnO<sub>2</sub> composite with more Sn–C chemical bonds. Liu and co-workers' [76] used Fenton reaction synthesis to produce Fe<sub>2</sub>O<sub>3</sub>/MWCNT and NiFe-LDH/MWCNT composite. The Fenton process uses H<sub>2</sub>O<sub>2</sub> and Fe<sup>2+</sup> to trigger oxidation of MWCNT which resulted in the attachment of hydroxyl functional groups on MWCNTs and the adsorption of Fe<sup>2+</sup> on the surface of the MWCNT via electrostatic bonding. The product suspension is subsequently sonicated, sintered and filtered to produce the composites. Fe<sub>2</sub>O<sub>3</sub>/MWCNT nanocomposite utilized as an anode for Li-ion battery exhibited high capacity, high

cyclability and rate performance. NiFe layered double hydroxide (LDH)/MWCNT employed as an oxygen evolution reaction (OER) electrocatalyst exhibited excellent chemical and mechanical stability and high oxygen evolution reaction electrocatalyst performance. The improved electrochemical performance of the  $\text{Fe}_2\text{O}_3$ /MWCNT and NiFe (LDH)/MWCNT composites was ascribed to improved electron and mass transfer cause from the conducting functionalized MWCNT scaffold's large surface area. High mechanical and chemical stability of the composites was caused by the strong interaction between the MWCNT and the metal oxide [76].

It has also been reported that CNTs produce a bridging effect when the composite is subjected to tensile loading which results in low electrical percolation threshold and enhanced fracture toughness. When CNTs are incorporated into metal oxide, the nanocomposite shows improved electrochemical performance, lower equivalent series resistance (ERS) and improve power density. Research has shown that CNT fillers can be used to modify membranes to enhance their thermal stability, flame resistance and electrical properties [77]. Some of the field applications of CNT/MO composites are schematically illustrated in Figure 4.

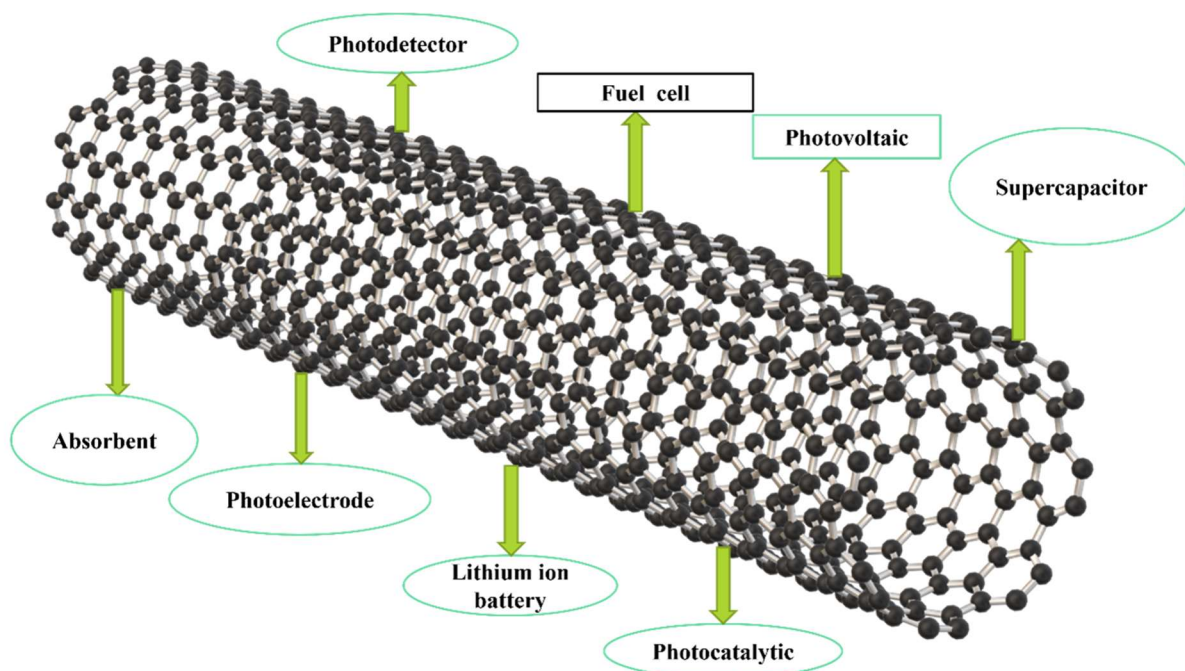


**Figure 4.** Application of CNT/metal oxide nanocomposite [78].

### 3. An overview of fuel cells

Fuel cells are energy systems that convert chemical energy to electrical energy. It involves the chemical reaction between fuel and oxidant to produce electricity, water, and heat energy. The efficiency of energy conversion in a fuel cell is accompanied by very low chemical emissions. It has been considered and studied as an alternative replacement for steam turbines, combustion engines and conventional batteries. This unique consideration is because of their high electrical efficiency, emission-free reaction, and high durability due to the absence of mechanical parts and no materials transformation during the operation [79]. Fuel cells have found application in automobile industries,

back-up power sources for buildings, small electronic and power plants. A fuel cell is made of two high porous electrodes (anode and cathode) and an electrolyte sandwiched in-between the electrodes which ensure that the two-half-cell reaction process takes place in isolation from each other. Figure 5 shows a schematic representation of fuel cell. The fuel source is supplied at the anode while the cathode is provisioned with oxygen (oxidant). Protons and electrons are generated in the anode; the electron migrates to the cathode through an external load, while the proton arrives at the cathode through the electrolyte. At the cathode, the electron combines with oxygen and proton to produce water [80]. These chemical reactions take place at the interface between the electrode and the electrolyte.

The general electrochemical reaction that take place at both the anode and the cathode are shown in Eqs 1–3:

At the anode



At the cathode



Overall chemical reaction

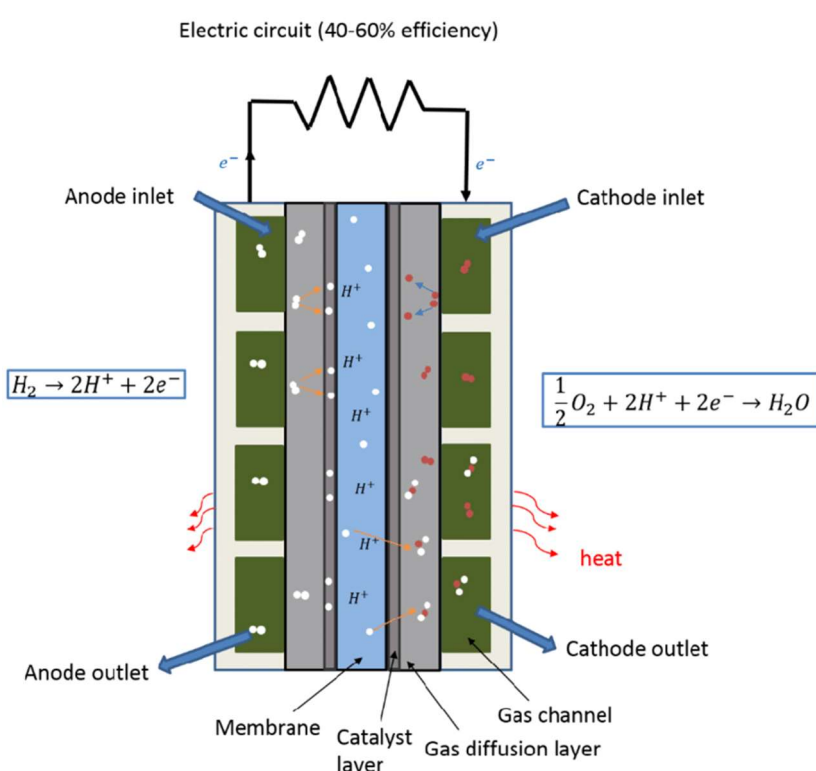


**Figure 5.** A typical representation of a unit fuel cell [81].

### 3.1. Type of fuel cell

Based on the type of electrolyte, fuel cells are classified into different types which includes alkaline fuel cell (AFC), polymer electrolyte membrane fuel cells (PEMFC), solid oxide fuel cells (SOFC), molten carbonate fuel cells (MCFC) and phosphoric acid fuel cells (PAFC). The characteristics of different types of fuel cells are summarized in the Table 1 below.

**Table 1.** Different types of fuel cells and their characteristic based on data extracted from works of literature [1,79,82–86].

Types of fuel cells	Electrolyte	Anode	Cathode	Charge carrier	Operating temperature (°C)	Fuel	Oxidant	Efficiency
AFC	Alkaline-potassium hydroxide	Ni	AC	$\text{OH}^-$	65–220	Hydrogen	Oxygen	60%–70%
Phosphoric acid fuel cell (PAFC)	Phosphoric acid			$\text{H}^+$	150–220	Hydrogen	Air	40%
PEMFC	Polymer membrane	Pt	Ni	$\text{H}^+$	40–80	Hydrogen	Air	60% with hydrogen, 40% with reformed fuel
Direct methanol fuel cell (DMFC)	Alkaline polymer membrane			$\text{H}^+$	20–90	Methanol	Air	40%
SOFC	Ceramic membrane ( $\text{Y}_2\text{O}_3\text{-ZrO}_2$ )	Ni & Yttria-stabilized zirconia (YSZ) cermet	Perovskite	$\text{O}^{2-}$	600–1000	Hydrogen, Methane	Air	55%–65%
MCFC	Alkali carbonate	Ni, Al, Cr alloy	Porous Ni	$\text{CO}_3^{2-}$	650–700	Hydrogen, Methane	Air	50%

## 4. Application of surface modified CNTs and CNTs composite in fuel cell

### 4.1. CNT as support material for platinum metal catalyst in fuel cell

Catalysts are a major component of PEMFC. It greatly determines the durability of the energy conversion system. Over the years Pt has been considered as one of the most suitable cathode catalyst materials for fuel cell application due to its electrocatalytic performance. However, the high cost of Pt, poor stability and poor Pt loading per unit area has hindered fuel cell commercialization [87]. For instance, the commercialization of PEMFC requires that Pt content in the 100 KW stack be reduced from 30 g to less than 10 g [88]. Nonetheless, the use of support materials can enhance the potential of the catalyst. A good catalyst support material should possess qualities such as: (i) a high specific surface area for distributing the catalyst, (ii) good electrochemical stability under fuel cell operation conditions, (iii) chemical stability at appropriate temperatures, and (iv) high electrical conductivity [89]. There has been substantial effort in research for good catalysts that will enhance electrocatalytic reaction kinetics and reduce the amount of Pt used for PEMFC. The efficiency of an electrocatalyst strongly depends on its particle size, particle distribution and the type of catalyst support [90]. The physical and chemical properties of the support material greatly affect the stability and dispersibility

of the metal catalyst which consequently influence the electrochemical performance of the catalyst [91]. Some of the catalyst support materials reported in literatures include carbon black, graphene, carbon gel, carbon nanofiber, reduced graphene oxide, CNTs and other forms of carbon [92–97]. Carbon black has been mostly employed as support material because of its electrical conductivity, large surface area and low cost. Pt-based nanoparticle supported on carbon black (Pt/C) has been utilized as cathode catalyst because of their good catalytic ability, low cost, and stability [98,99]. Pt/C showed. The major challenge in the commercialization of Pt/C cathode catalysts is their gradual loss of performance over time. Some of the causes of this degradation include: (i) carbon support corrosion, (ii) sintering of catalyst particles, and (iii) dissolution of the catalyst [100]. The dissolution of Pt is typically negligible at both low and high potentials. At low potentials, noble metal dissolution in acid is minimal. Conversely, at high potentials, exposure to air results in the formation of PtO, which acts as a protective film, preventing further dissolution of Pt particles. However, at intermediate potentials, Pt experiences a high rate of dissolution in acid [101–103]. The carbon support used in electrocatalysts often reacts with oxygen and/or water at elevated temperatures, forming CO and CO<sub>2</sub>, which are released from the cell as gases. Carbon corrosion also occurs during cell start-up and shutdown, which happens at high potentials (1.1–1.5 V) [100]. The oxidation of carbon renders the cathode surface hydrophobic, leading to poor mass diffusion. As carbon corrodes, noble metal agglomeration increases, causing a rise in ohmic resistance, structural collapse, and eventual degradation of electrochemical active surface area (ECSA) [101,104–106]. The discovery of CNTs and the study of the characteristics of CNTs rapidly increased the interest of researchers to give more consideration to the use CNTs as a more popular alternative material for catalyst support. CNTs have a unique structure, which provides them with high surface area, high electrical conductivity and chemical stability which results in an improved chemical interaction between the noble metal catalyst (Pt) and the CNTs. CNTs have fewer impurities than carbon black that can poison the metal catalyst and are free of deep cracks that limit catalytic activity. When compared to other forms of carbon, CNT are completely distinct due to their tubular structure which makes a sort after support material for heterogeneous catalysis [107]. CNTs have high resistance to fouling when compared to carbon fiber which makes it a potential material for membrane electrode assembly (MEA) [108]. CNTs (both SWCNT and MWCNT) have been widely explored as carbon nanostructure catalyst support in fuel cells. Pristine CNTs are chemically inert and hydrophobic which makes it very difficult for metal nanoparticle attachment [109,110]. Hence CNTs used in a PEM fuel cell are first modified via doping to make it more hydrophilic and enhance the dispersion of metal catalyst particles. For instance, Tang et al. [111] Pt nanodot deposited on CNT prepared by in situ CVD on carbon paper was used as a gas diffusion layer (GDL) and the catalyst delivered a high-power density of 595 mW·cm<sup>-2</sup> with Pt loading of 0.04 mg·cm<sup>-2</sup>. Microstructural examination revealed a well-dispersed Pt nanodot on highly porous CNT. Jha et al. [112] prepared SWCNT functionalized with carboxylic acid SWCNT-COOH as catalyst support for PEMFC with a Pt group metal loading of 0.16 mgpt/cm<sup>2</sup> which was below the benchmark value of 0.125 mgpt/cm<sup>2</sup> set by US department of energy in 2017. In the study, the SWCNTs were synthesized by the electric arc method followed by functionalization using conc. HNO<sub>3</sub> as oxidizing agent to introduce –COOH functional group on the surface of the SWCNT. Subsequently, Pt nanoparticles were attached to the –COOH functionalized SWCNT by in situ reduction process using ethylene glycol. Lin et al. [113] Prepared MWCNT functionalized with citric acid and used it as catalyst support for Pt. The study revealed that Pt/MWCNT nanocomposite as catalyst drastically reduced the MEA degradation as strong bond between Pt nanoparticle and MWCNT functionalized with citric acid (CA) was obtained. Tian [114]

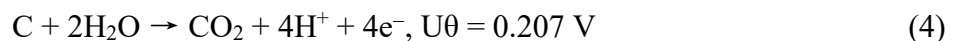
prepared vertically aligned carbon nanotube (VACNT) grown on aluminum (Al) via enhanced chemical vapor deposition. The CNT/Al was used as catalyst support in PEMFC. Pt nanoparticle was hot pressed into VACNT/Al and was able to achieve a great Pt reduction to  $35 \mu\text{g}\cdot\text{cm}^{-2}$ . Zhang et al. [115] prepared Pt/CNT as electrocatalyst support for PEMFC. The vertically aligned CNT was first purified via plasma treatment and functionalized with poly (dially dimethyl ammonium) chloride. Thereafter, Pt nanoparticles were electrostatically adsorbed on the surface of aligned CNT. The Pt/CNT was hot pressed into Nafion 115 membrane electrode. Pt/CNT used as cathode catalyst support for oxygen reduction reaction (ORR) exhibited high mechanical stability, high electronic conductivity, high gas permeability and enhanced rapid water removal from the cathode than Pt/unaligned CNTs catalyst support. Guo and Li [116] prepared Pt-SWCNT composite as an electrocatalyst for methanol oxidation and studied the electrocatalytic and cyclic stability of the composite. The authors employed three stages in the preparation of the composite. Firstly, the oxide functional was introduced on the sidewalls and the ends of CNTs by treating the CNTs with 0.5 M NaSO<sub>4</sub> solution. Secondly, cyclic voltammetry at potential window of +0.3–1.3 V was used on Pt octahedra complexes from 2.5 mM PtCl<sub>4</sub> + 0.1 M K<sub>2</sub>SO<sub>4</sub>. Finally, the Pt complexes formed on SWCNT were reduced to Pt nanoparticles using 0.1 M H<sub>2</sub>SO<sub>4</sub>. The result showed that Pt-SWCNT composite exhibited high electrocatalytic activity and good stability for the oxidation of methanol. The excellent performance of the composite was attributed to the nanoparticle size of the Pt and the good dispersion of the noble metal on the SWCNT surface.

Besides using carbon as support for noble metals such as Pt, research has also explored the use of carbon-based metal-free (CBMF) electrocatalysts for the ORR in PEMFC, gaining attention due to their potential to exhibit improved ORR activity and electrochemical stability compared to Pt-based electrocatalysts [117]. This is attributed to the presence of active sites both in the basal plane and edges of the carbon material. For instance, graphene-based catalysts, owing to their 2D structure and electron conductivity, enhance electron mobility through both the basal and edge regions of the catalyst. The use of CNTs or graphitized CNTs increases exposed active edge sites and causes the ORR to proceed with a more positive onset potential. Carbon materials exhibit high electron density and diffusion current density, with more rapid electron transport at the edges than on the plane due to the low contact resistance exhibited at the edge sites of graphene [117,118]. To address the challenge of chemical inertness of carbon material, functionalization and doping of carbon with heteroatoms has been shown to create defects and alters the surface energy, atomic structure and enhance the reactivity of carbon. Doping carbon materials with heteroatoms further enhances the ORR and hydrogen evolution reaction (HER) activity due to electron interaction between adjacent carbon atoms and the heteroatom (e.g., N, B, P, and S) [117,119]. For example, boron doping of pristine CNTs transforms semiconducting carbon nanotubes into conductive tubes by lowering the Fermi energy level into a valence band, thus altering the stiffness and crystallinity of CNTs. The presence of boron dopants increases the number of defects on the CNT walls, resulting in increased reactivity, making it viable as an electrocatalyst [120]. In the study conducted by Jarrais et al., the doping of graphene flakes and MWCNTs with N, P, S, and B via a mechanochemical process followed by subsequent thermal treatment was investigated. The assessment revealed that the doped carbon materials exhibit improved chemical reactivity than their pristine counterpart and can be utilized as CBFM electrocatalysts for 4-Nitophenol reduction [121]. Akula et al. examined the structural properties and electrochemical performance of MWCNT co doped with N and F (N-F/MWCNT). It was revealed that doped MWCNTs transformed to folded graphene structure with numerous active open edge sites that enhance ORR. The N-F/MWCNTs electrocatalyst exhibited no degradation after 10000 cycles in acidic medium. The excellent durability and high ORR

activity of N-F MWCNTs electrocatalyst was attributed to the high charge dislocation density on CNT matrix caused by the wide electronegativity gap between the N and F [122]. A comparison between nitrogen doped carbon material and fluorine doped carbon material reveals that F-doped carbon exhibit better ORR activity and corrosion resistance than N doped carbon both in basic, acidic environment and high potential. It was also reported that F-doped carbon showed improved catalyst resistance to degradation during start up and shut down operation of the PEMFC. The outstanding performance of F doped carbon was due to its high electron affinity and ability to effectively alter the electronic band structure of carbon [123].

#### 4.2. CNT as corrosion inhibition material in PEMFC

Under PEMFC operating condition carbon support present in the Pt/C electrode catalyst is electrochemically unstable and usually undergoes carbon corrosion at open circuit potential (OCP) near 1 V. Also, when gas flows are turned on and off during start-up and shut-down condition, reverse current situations, and extraordinarily high potentials of more than 1.5 V at the cathode may result to corrosion damage [100]. Although, the gas exchange events only last for a short while, the accumulation of it reduces the lifespan of a fuel cell system. It has been proven that extensive corrosion causes the porous cathode microstructure in PEMFCs to collapse, and it is assumed that this is the cause of the substantial mass-transport voltage losses seen in polarization data [124]. The main side effects of carbon corrosion on fuel cell electrodes are the dissociation and deactivation of Pt nanoparticles from their support and the collapse of the porous framework, which restricts the mass transfer of reactants (oxygen and proton) and generate water in the cathode electrode [125–127]. The electrochemical carbon degradation is represented by the reaction in Eq 4:



Before oxidation to carbon dioxide, various carbon-oxide surface constituents may form. Also, catalytic interaction between the electrocatalyst, carbon-oxides, and ionomer occur which influences the kinetics, potentially accelerate the corrosion reaction. This corrosion is frequently accompanied by a loss in ECSA, unusual accumulation of negative charges on the surface of the electrode [124].

Research has shown that the utilization of modified CNTs as catalyst support reduces carbon corrosion especially at high potential. Oxygen and nitrogen functionalized multiwall carbon nanotube as support for Pt catalyst exhibited improved ORR electrochemical performance and durability over commercial Pt/C [126]. Numerous studies have investigated the doping of CNTs, either through substitution or endohedral doping with elements such as K, I, Cl, Li, and N. This modification results in CNTs with enhanced electrical conductivity and improved dispersion, both in solution and during CVD growth processes [128]. For instance, Karthikeyan et al. [129] studied the carbon corrosion stability of Pt deposited on nitrogen doped functionalized MWCNT support (N-f-MWCNT) and nitrogen doped functionalized MWCNT/few layers graphene (FLG) hybrid support (N-f-(MWCNT/FLG)). The MWCNTs were synthesized with conc.  $HNO_3$  and  $H_2SO_4$  (1:3 (v/v)) via ultrasonication. The doping was done using high temperature nitrogen plasma treatment and finally Pt incorporation in the modified catalyst supports via modified polyol reduction technique to develop Pt/N-f-MWCNT and Pt/N-f-(MWCNT + FLG) electrocatalyst with Pt loading of 30 wt.%. The electrochemical investigation result revealed that Pt/N-f-MWCNT and Pt/N-f-(MWCNT+FLG) utilized as electrocatalyst in PEMFC showed about 30% enhancement in durability in carbon corrosion durability test, mass specific

activity (MSA), area specific activity and an overall improvement on ORR performance than what was obtained with Pt/C catalyst. The author attributed the outstanding performance of electrocatalyst to the presence of nitrogen and oxygen functional group which greatly enhanced the corrosion resistance of Pt/N-f-MWCNT and Pt/N-f-(MWCNT + FLG) at wide potential range and extensive graphitization that occurred during nitrogen plasma treatment. The high electrostatic attraction of oxygen and nitrogen functional groups on carbon support structure exist as strong binding sites for Pt atoms, leading to reduced particle agglomeration all through the extended cycles. In a recent study by Kanninen et al. [126] carbon corrosion performance of Pt supported on MWCNT, and nitrogen modified MWCNT was investigated as fuel cell electrode in PEMFC and compared with commercial Pt/Vulcan catalyst. The result showed that Pt/MWCNT and Pt/N-MWCNT exhibited high corrosion stability than the conventional Pt/Vulcan, with initial corrosion rate of 1.1, 3.4 and 4.7  $\mu\text{g C} (\text{mg Ctot})^{-1}/\text{cycle}$  respectively. The carbon corrosion inhibition properties of popular electrocatalyst and CNT based electrocatalyst are listed in Table 2.

**Table 2.** Carbon corrosion durability study of some electrocatalyst.

Electrocatalyst	Carbon loss	Potential range (V)	Atmosphere	Electrolyte	Number of cycles	Temperature	ECSA retention (%)	Ref.
Pt/Vulcan XC 72		1.0–1.5	$\text{N}_2$	0.1 M $\text{HClO}_4$	60000		36.3	[130]
Pt/Vulcan XC 72		0.85–1.4		0.1 M $\text{HClO}_4$	1800		31.4	
Pt/Ketjen black		1.0–1.5	$\text{N}_2$	0.1 M $\text{HClO}_4$	60000		2.1	[130]
Pt/nano graphite		0.85–1.4		0.1 M $\text{HClO}_4$	1800		53.1	[131]
Pt/MWCNT		0.9, 7 days	$\text{N}_2$	0.5 M $\text{H}_2\text{SO}_4$		60 °C	63.0	[132]
Pt/N-f-MWCNT		1.0–1.5	$\text{N}_2$	0.1 M $\text{HClO}_4$	60000	60 °C	91.5	[129]
Pt/N-f-(MWCNT+FLG)		1.0–1.5	$\text{N}_2$	0.1 M $\text{HClO}_4$	60000	60 °C	90.4	[129]
Pt/MWCNT	29% after 70 cycles	0.1–1.6	$\text{N}_2$		70	80 °C	100.0	[126]
Pt/N-MWCNT	28% after 70 cycles	0.1–1.6	$\text{N}_2$		70		87.0	[126]
Pt/Vulcan	30% after 70 cycles	0.1–1.6	$\text{N}_2$		70		18.0	[126]

#### 4.3. Pt-alloy with CNTs as electrocatalyst

In the past few years, researchers' interest in Pt-alloy catalyst support on CNTs has grown as a result of this nanocomposite material's exceptional ability to boost fuel cell performance and reduce the overall cost of the fuel cell [133]. A good electrocatalyst characteristic requires that the binding energy between the catalyst and the reaction species should not be too strong. Hence, the introduction of another metal (rare earth and/or transition metal) will alter this bonding strength and increase the durability and electrocatalytic performance [134,135]. Borghei et al. [136] compared the performance of different carbon support such as MWCNTs, graphitized carbon nanofiber (GNF) and Vulcan on PtRu-alloy catalyst. PtRu/MWCNT, PtRu/GNFs and PtRu/Vulcan electrocatalyst delivered 20.0, 13.1 and 3.5  $\text{mW}\cdot\text{cm}^{-2}$  respectively. While PtRu/Vulcan had the highest power density which showed the highest durability as it retained 91% of its power density after 72 h. The outstanding electroactivity of PtRu/MWCNT electrocatalyst was due to the unique structure of functionalized MWCNTs that improve the electron mobility in the electrode. However, PtRu/MWCNT experienced high current decay in the 72 h durability test which was linked to loss and migration of bigger particles from the

support to the ionomer, which would mean that they lost contact with the support and stopped participating in the electrochemical reaction. Lopez-Rosas et al. [137] prepared Pt-Ni/CNT cathodic catalyst for ORR using ethylenediamine. CNT was functionalized with  $H_2SO_4/HNO_3$  (1:3 molar ratio). Ni was deposited on the surface of CNT via direct chemical reduction using ethylenediamine. Pt-Ni/CNT was synthesized by in situ electrolytic displacement reaction. Pt-Ni/CNT cathode catalysts with low Pt and Ni content of 2.23 and 1.98 wt.% respectively show an improved electrocatalytic performance and power density for PEMFC. At high metallic content, MEA poisoning occurs as de-alloyed metal deposit on the MEA surface and prevents fuel diffusion across the membrane. Wang [138] synthesized 3D graphite oxide-exfoliated carbon nanotube (GO + e<sup>-</sup>CNT) via homogeneous mixing and used it as support for the Pt-Pd catalyst. The e<sup>-</sup>CNT served as a carbon spacer and prevented the restacking of graphene oxide. Pt-Pd-GO + e<sup>-</sup>CNT was fabricated using the chemical co reduction method. Garapati et al. [139] developed novel partially exfoliated CNT (PECNT) cathode support on Pt<sub>3</sub>Sc alloy catalyst for PEMFC. The CNTs was synthesized by CVD and partially oxidized using KMNO<sub>4</sub> via modified hummers method and further annealed to reduce the O-functional group to produce partially exfoliated carbon nanotube (PECNT). The Pt<sub>3</sub>Sc was then dispersed on PECNT surface by polyol technique to form Pt<sub>3</sub>Sc/PECNT cathode electrocatalyst. Through half-cell investigations, it was reported that Pt<sub>3</sub>Sc alloy was responsible for accelerated ORR with faster kinetics while PECNTs' mesoporous structure and high pore volume reduced mass transfer losses. PECNT incorporation drastically reduced the cathode catalyst loading. Pt<sub>3</sub>Sc/PECNT delivered a high-power density of 760 mW·cm<sup>-2</sup> at 60 °C operating temperature due to the high mass activity of the electrocatalyst. Pt<sub>3</sub>Sc/PECNT electrocatalyst showed excellent durability and efficiency. The improved electrocatalytic performance of Pt<sub>3</sub>Sc/PECNT was attributed to the synergistic effect of Pt<sub>3</sub>Sc alloy nanoparticles and PECNT support which has 1-dimensional CNT and 2D graphene morphology and can adsorb oxygen with less binding energy than Pt. He et al. [140] decorated MWCNT with bimetallic Pt-Ru nanoparticles to produce Pt-Ru/MWCNT composite via electrochemical deposition for use as an electrocatalyst in DMOFC. The introduction of Ru reduced the poisoning effect of CO on the Pt catalyst, which is the by-product of methanol electrooxidation. The MWCNT was oxidized with 0.5 M  $H_2SO_4$ . Pt:Ru ratio of 4:3 in the composite gave the best electrocatalytic activity for methanol oxidation and better stability than Pt-MWCNTs.

The heteroatom functionalization of CNT is one of the ways to influence the physiochemical properties of CNT. Heteroatom such as nitrogen alters the electron density and increases the catalytic activity of the material [141]. Most of the Pt/CNT electrocatalysts, despite showing exceptional performance in alkaline media, showed poor performance in acid media which limits the utilization in fuel cells. Researchers are paying more interest to closing this gap by doping CNT with one or two heteroatoms such as nitrogen [142], phosphorus [143] and sulphur [144]. Such modification of CNT is expected to increase the synergistic effect and catalytic activity of the electrocatalyst and consequently enhance performance in both basic and acidic media. Most of these studies used precursors such as polymer resin, amine, and organic polymer as dopants to introduce these heteroatoms into CNTs. The hydrophilicity of carbon-based materials can be increased by the formation of nitrogen groups on their surface. The addition of nitrogen groups strengthens the bond between the catalyst and the support, increasing the activity and catalytic stability while decreasing the Pt loading [145]. For instance, Shi et al. [146] prepared Nitrogen-doped MWCNT and supported it on Pt-Co catalyst via pyrolysis using zeolitic imidazolate frameworks (ZIF) to produce Pt-Co/N-MWCNT electrocatalyst. The comparison of Pt-Co/N-MWCNT and Pt/C electrocatalyst

showed that Pt-Co/N-MWCNT electrocatalyst has an improved power density of  $690 \text{ mW}\cdot\text{cm}^{-2}$  at  $70^\circ\text{C}$ , very low Pt loading of 0.12 mg and good durability while Pt/C under same condition delivered power density of  $560 \text{ mW}\cdot\text{cm}^{-2}$ . The improved performance of the Pt-Co/N-MWCNT electrocatalyst was attributed to the proper dispersion of Pt-Co alloy on N-MWCNT which also inhibited the CO poisoning. The N-MWCNT increased the ORR. Mardle et al. [143] prepared Pt nanorod catalyst supported on well-aligned nitrogen doped CNTs which was used to develop thin film electrodes for PEMFC. The nitrogen doping was done using screen plasma treatment, while the growing of the Pt nanorod was done via PECVD. When compared to standard Pt/C catalysts, an increase in power density was achieved with less than half of the Pt loading of the Pt/C catalyst. The authors suggested that the thin open catalyst layer was responsible for the improved mass transfer performance. It is also confirmed that the nanorods' high structural stability and the enhancing effects of the N functionalized CNT support result in improved durability. Roudbali et al. reported the improved performance of Pt/N-MWCNTs over Pt/MWCNT composite cathode electrocatalyst for ORR in PEMFC. In the study, the author introduced N on the surface of the MWCNTs using diethylenetriamine (DETA), triethylenetetramine (TETA), and malononitrile (MN) precursors. The nitrogen functional group on CNT's surface enhances the alkaline characteristic of the CNT. These alkaline sites enhance the interaction and bonding of Pt nanoparticles on the support and allow the uniform dispersion of Pt on N/MWCNT support. The N-functional group on the CNT greatly influences the particle size of the catalyst. The strong interaction between the N-MWCNT and the Pt during nucleation and catalyst production was attributed to the lone electron pair present in the N-group. The authors concluded that Pt supported on N-doped MWCNT (Pt/N-MWCNT) showed greater electrocatalytic behaviour and higher stability than Pt/MWCNT [147]. Hoque et al. [144] utilized modified solvothermal technique to synthesize a sulphur-doped carbon nanotube (S-CNT) supported on Pt nanowire (Pt/S-CNT) to fabricate an electrocatalyst with weblike 3D architecture. The 3000-cycle acceleration durability test carried out on Pt/S-CNT revealed that the composite electrochemical activity retention, stability, and mass activity was much higher than commercial Pt/C catalyst. Pt/S-CNT delivered a specific activity of  $1.61 \text{ mA}\cdot\text{cm}^{-2}$  whereas Pt/C has  $0.24 \text{ mA}\cdot\text{cm}^{-2}$ . These enhancements were attributed to the fewer surface defect present in the composite, the strong interaction of sulphur functional group in S-CNT and the Pt nanoparticles which resulted to strong bonding of the Pt nanowires and improved stability. However, the ORR is reduced drastically by Pt/S-CNT cathode catalyst. The structure of CNTs can also be changed by co-doping with heteroatoms, which increases the catalysts' activity and stability [148].

CNT nanocomposite has also been employed as a noble metal-free electrocatalyst in fuel cells. For instance, Zhao prepared manganese cobalt oxide/nitrogen-doped multiwalled carbon nanotube  $\text{MnCo}_2\text{O}_4@\text{NCNTs}$  with superior ORR activity, high current density, and durable and tunable catalytic activity for OER with a very low overpotential of 0.930 V [149]. Dual-phase spinel dp- $\text{MnCo}_2\text{O}_4/\text{CNT}$  hybrid composite performed excellently well as OER and ORR catalysts.  $\text{MnCo}_2\text{O}_4/\text{CNT}$  composite was stable after 768 h of charge-discharge process whereas Pt/C retain stability only for 108 h of charge-discharge processes of the Zn-air battery [150]. In another study, Xing et al. [151] synthesized bimetallic nanocomposite by the combination of Manganese and Vanadium with nitrogen/sulfur doped MWCNT. The Mn/V-functionalized N/S doped MWCNT composite when compared with commercial Pt/C showed increased electrical conductivity, improved stability and enhanced ORR/OER electrocatalytic activity. Iron single atom (FSA) supported on CNT synthesized by template free method and studied as a possible replacement for Pt/C cathode catalyst for high temperature PEMFC. The study revealed that FSA with 3.5 wt.% Fe content showed half wave potential of 0.8 V in 0.1 M

$\text{HClO}_4$  electrolyte and improved ORR performance compared to commercial Pt/C. the excellent performance was attributed to the high conductive network of CNTs and the high-density atomic site present in the composite. The FSA/CNT composite also delivered a high-power density of  $266 \text{ mW}\cdot\text{cm}^{-2}$  and high electrochemical stability at  $240^\circ\text{C}$ . Also, CNT was responsible for the enhanced electrocatalytic performance and corrosion resistance. This was in support of the report by Li et al. CNTS support on FSA catalyst increased charge transfer and improved ORR activity and the overall durability of the catalyst particularly at elevated overpotential [152].

Moreso, the addition of metal oxides, such as  $\text{MoO}_x$ ,  $\text{RuO}_2$ ,  $\text{NbO}_2$  and  $\text{TiO}_2$ , to Pt/CNT has been found to enhance electrochemical stability and reduce carbon corrosion, particularly under harsh working conditions, thereby extending cycling longevity and open circuit potential (OCP). This addition of metal oxides provides a robust interfacial bond between the noble metal and the carbon, improving the catalytic band for the ORR [153]. Pt nanoparticles deposited on NbO and supported on MWCNTs exhibited increased durability under accelerated stress testing (AST) compared to Pt/CNT during load cycling, start-up, and shut-down processes. The Pt/NbO/CNT composite demonstrated high electroactivity of  $57 \text{ mA}\cdot\text{mgPt}^{-1}$  and exceptional stability at  $0.15 \text{ mg}\cdot\text{cm}^{-2}$  Pt loading. The electrocatalyst delivered a power density of  $772 \text{ mW}\cdot\text{cm}^{-2}$  and experienced only a 4% loss in power density when operated at a temperature of  $80^\circ\text{C}$ . The overall excellent performance of the hybrid composite was attributed to the effective adherence of Pt nanoparticles on the CNT/NbO support [154].

#### 4.4. Functionalized CNT-polymer composite membrane for PEMFC

The proton exchange membrane is one of the major components of PEMFC. It allows the passage of protons from the anode to the cathode. There are different types of membranes which include membranes based on (i) poly (perfluoro sulfonic acid) such as Nafion-based membrane, (ii) membrane based on sulfonated aromatic polymer such as sulfonated poly (ether ether ketone) (SPEEK) and poly (arylene ether ketone) (SPAEK), (iii) membrane based on heterocyclic aromatic polymer such as derivative of polybenzimidazole (PBI) [155]. Nafion-based membranes have been the most studied and successfully utilized for fuel cells due to their good mechanical, thermal and chemical properties. Nafion has low proton conduction resistance and rapid oxygen reduction potential. They find applications at temperatures below  $90^\circ\text{C}$  and operate under humid conditions. The ionic conductivity of Nafion is greatly influenced by the water content, that is the higher the water content of the membrane the higher the ionic conductivity [156]. However, excessive water within the membrane can lead to water flooding, an undesirable phenomenon particularly for PEMFCs operating at high current densities, high temperature and humidity levels. The hydration of the membrane consequently leads to loss of the functional group which is responsible for proton conductivity. Therefore, it is not feasible to continuously increase the water content to achieve higher ionic conductivity. Hence Nafion membrane based PEMFC is usually operated at low temperature (below  $90^\circ\text{C}$ ) [156,157]. All the above-mentioned membrane was found to still suffer some drawback ranging from acid leaching, operating temperature, and poor proton conductivity at elevated temperature. These limitations had prompted a shift in research focus to the introduction of inorganic and/or organic fillers into the bulk polymer materials to produce mixed matrix composite membranes that will combine the benefiting properties of the constituent and deliver a more efficient proton exchange membrane. Some of the fillers that have been studied include CNT, metal-organic framework, and ionic liquids. Among these filler materials, CNTs have been greatly considered because of their outstanding mechanical properties,

large surface area, low density, and high aspect ratio [65,158]. When CNT is used as a filler strong interaction is observed between the CNT and the Nafion polymer chain which effectively will aid packing and significantly improve the gas diffusion [159]. For example, Asgari et al., [160] prepared Nafion/histidine functionalized CNT (Nafion/Im-CNT) composite membrane for application in DMFC. The surface modification of the CNT with the imidazole acid group produced an electrostatic interaction at the interface of IM-CNT and Nafion. The membrane exhibited an increased power density and high proton conductivity compared to Nafion 117. Steffy et al. [161] fabricated Nafion/sulfonic acid-MWCNT (Na/s-MWCNT) hybrid membrane with low humidity for PEMFC application. The functionalization of the MWCNT filler with sulfonic acid increased the number of  $-\text{SO}_3\text{H}$  groups on the surface, which enhance the compatibility of the s-MWCNT with the Nafion matrix. The incorporation of the s-MWCNT resulted in enhanced mechanical and thermal stability of the hybrid membrane. Moreso, the hydrophilic property of s-MWCNT improved the proton conductivity and the water intake capacity of the Na/s-MWCNT. Na/s-MWCNT employed as a membrane in PEMFC delivered higher power density than pristine Nafion membrane. Kim et al. [162] prepared sulfonated deblock copolymer (s-DBC)/sulfonated CNTs (s-DBC/s-CNT) composite membranes by solution casting method. The study was carried out with different wt.% of s-CNT fillers (0, 0.5, 1, 1.5 and 2 wt.%). The incorporation of s-CNT improved the water intake capacity and proton conductivity of the composite membrane. The high volume of sulfonic acid group on the membrane was responsible for the increase in the conductivity of the composite. The addition of the filler enhanced the thermal stability and mechanical properties of the composite membrane. This increase was due to effective interfacial interaction between the s-CNT and the polymer backbone of the composite through  $\pi-\pi$  interaction and hydrogen bonding which inhibit the mobility of the polymer chain segment. However, at higher filler content (S-DBC/s-CNT-2 wt.%) the mechanical property of the composite membrane drastically drops which was attributed to phase separation and agglomeration. Chemical degradation is regarded as one of the most serious membrane degradation processes that can take place during actual fuel cell operations. Peroxide ( $\text{HOO}^-$ ) and hydroxyl ( $\text{HO}^-$ ) radicals produced by the incomplete ORR at the cathode have been identified as the main causes of the considerable degradation of membrane components. The normal process of membrane degradation begins with the addition of radicals to the aromatic backbone, which sets off a series of chain reactions that continue until the entire polymer backbone is broken down [163]. s-DBC/s-CNT composite membrane when subjected to Fenton's test showed high chemical stability and resistance to oxidation. The incorporation of s-CNT fillers retarded the deterioration process. By first reacting with the radicals, the s-CNTs served as barriers that stopped the polymer's backbone from breaking down too quickly. The few oxygens functional groups that SCNTs contain on their surface, which were created during their initial oxidation before being sulfonated, interacted with the incoming radicals, and defended the polymer backbone from the attacks. Also, the C–F bond from the hydrophobic oligomer was also a crucial factor in the defense of membranes against radicals was the robust, inert. The s-DBC/s-CNT-1.5 composite membrane had the best enhanced mechanical, electrochemical properties, proton conductivity and thermal stability than pure s-DBC and Nafion 117. s-DBC/s-CNT-1.5 delivered maximum power density of  $171 \text{ mW}\cdot\text{cm}^{-2}$  at load current density of  $378 \text{ mA}\cdot\text{cm}^{-2}$ . Table 3 shows a summary of the electrochemical, mechanical, and chemical stability of the pristine s-DBC and s-DBC/s-CNT composite membranes.

**Table 3.** A summary of the electrochemical, mechanical, and chemical stability of the pristine s-DBC and s-DBC/s-CNT composite membranes of different wt.% s-CNT composition [162].

Properties	Pristine s-DBC	s-DBC/s-CNT- 0.5	s-DBC/s-CNT- 1	s-DBC/s-CNT- 1.5	s-DBC/s-CNT- 2
Young modulus (MPa)	625	625		1262.5	420.8
Tensile strength (MPa)	26.8	26.8		45.4	22.5
Elongation at break (%)	6.4	6.4		9.6	6.4
Oxidation stability (%) RW	90.5	91.0		92.6	93.2
Water uptake (%)	11.5	16.2	21.0	29.1	27.5
Swelling in volume ratio (%)	11.8	18.7	24.2	31.4	29.2
IEC (meq/g)	1.21	1.39	1.58	1.91	1.72
Power density (mW/cm <sup>2</sup> )	119			171	

Ahmed et al. [164] synthesized sulfonate functionalized MWCNTs by 1,3-propane sultone (PS) method and distillation polymerization (DP) method respectively and incorporated them into chitosan (CS) to develop chitosan/MWCNTs (CS/s-MWCNT) nanocomposite membrane for PEMFC. It was reported that the presence of the sulfonated MWCNTs homogeneously dispersed in the CS matrix inhibited the mobility of the CS polymer chain which resulted in enhanced thermal and mechanical properties of the composite compared to pure chitosan. The addition of functionalized MWCNT inhibit and terminated crack propagation in the composite membrane. The water uptake and swelling decrease with the introduction of s-MWCNT from (0 to 5 wt.% of the s-MWCNT) of the CS/s-MWCNT membrane. An increase in water uptake in CS caused methanol oxidation and a reduction in mechanical stability due degradation of the chitosan chain [165]. CS/s-MWCNT-5 wt.% composite exhibited an improved proton conductivity of  $0.025 \text{ S}\cdot\text{cm}^{-1}$  compared to pristine CS which was  $0.011 \text{ S}\cdot\text{cm}^{-1}$ . This development was attributed to the formation and electrostatic interaction between the  $-\text{NH}_2$  functional group from CS and the  $-\text{SO}_3\text{H}$  functional group from sulfonated MWCNT. The authors investigated the effect of the two methods of functionalization (DP@s-CNT and PS@s-CNT) on the properties of the MWCNT and the performance of the nanocomposite membrane. Sulfonated functionalized MWCNT showed a slight weight reduction in the thermal stability at  $500^\circ\text{C}$  as shown in Figure 3d, when compared with pristine MWCNT due to the decomposition of the polymer grafted chains. However, at  $750^\circ\text{C}$ , the char residue yield of the DP@s-CNT and PS@s-CNT were 48.6 and 28.87 wt.% respectively due to enhanced char formation of MWCNT by the functionalization which was higher than pristine MWCNTs that was 15.42 wt.%. Morphological examination revealed that pristine MWCNT showed clear tubular structure while sulfonated MWCNT by 1,3-propane sultone method showed homogeneous distribution of granular structure of sulfonated group along the MWCNTs. Sulfonated MWCNTs by distillation polymerization method displayed grafted polymers which show strong electron affinity as can be seen in Figure 6a–d. The fabricated CS/s-MWCNT composite membrane exhibited improved mechanical and thermal stability.

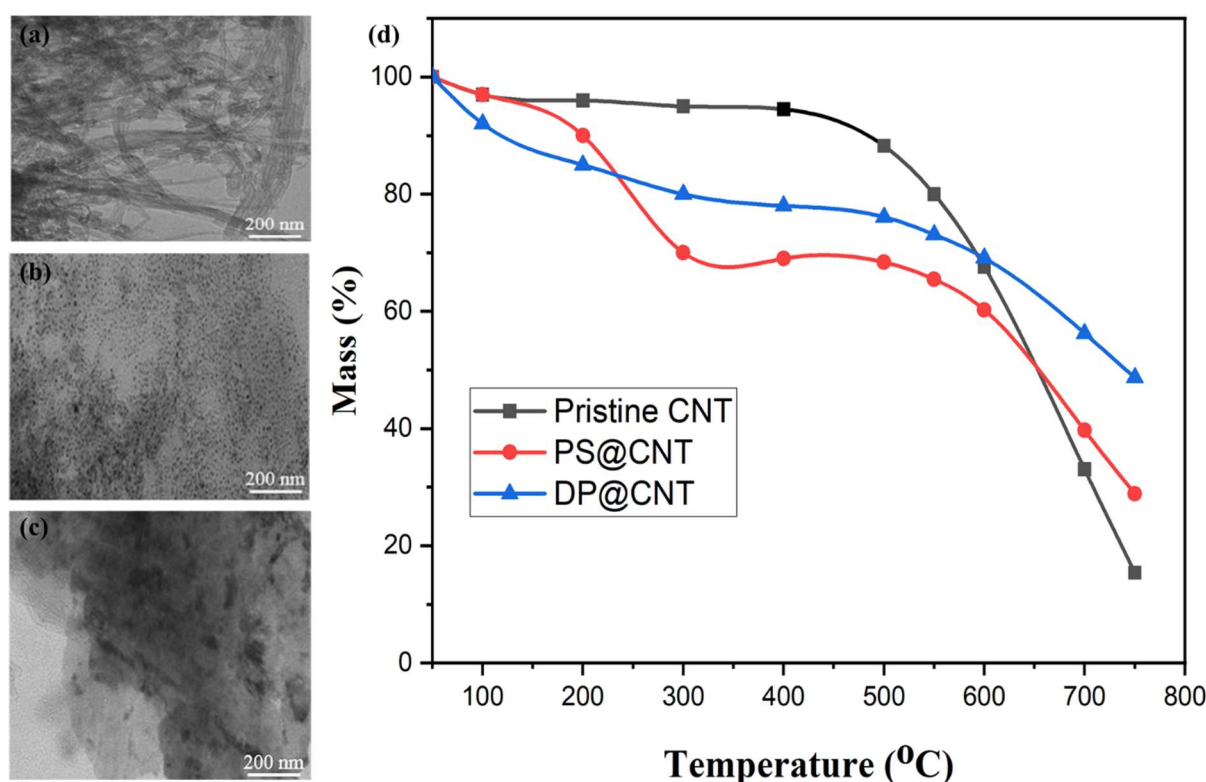


**Figure 6.** TEM micrograph of (a) pristine CNT, (b) PS@CNT, (c) DP@CNT and (d) thermal gravimetric analysis curve of pristine CNT, PS@CNT, and DP@CNT [164].

Functionalization of CNT using histidine produces an increased electrostatic interaction between Nafion membrane and CNTs, which when deployed as a proton exchange membrane (PEM) will exhibit high proton conductivity, electrochemical performance, and reduced methanol permeability. Asgari et al. examined the performance of Nafion supported by 0.5 wt.% histidine modified CNTs (Im-CNT) as membrane for DMFC application. The result obtained when compared to commercial Nafion showed that Nafion/Im-CNT exhibited enhanced power density, water uptake capacity and low methanol crossover [160]. SWCNT covalently functionalized with naphthoic acid group from amino acid and supported on Nickel bis-diphosphine complex and deployed as anode catalyst in hydrogen biofuel cell PEMFC. The composite showed high interfacial electron transfer kinetics and potential to be utilized as hydrogen oxidizing electrocatalyst [166].

#### 4.5. CNT-based nanocomposite as bipolar plate used in the fuel cell

Bipolar plates (BPs) are one of the key components of PEMFC. They are used in joining several single cells together while collecting and moving the current generated from one cell to another. They ensure the even distribution of reactant gas on the electrode and the removal of water and unused gases [167,168]. Therefore, a good BPs material must possess high corrosion resistance, low cost, good thermal and electrical conductivity, ease of machining, low gas permeability, high mechanical stability and lightweight [167,169]. Graphite has been the most widely employed material for BPs because of its good electrical conductivity ( $104 \text{ S}\cdot\text{cm}^{-1}$ ). However, it is expensive and has low ductility. Metallic BPs have been considered in the past decades because of their good electrical conductivity

and structural properties. But the high humidity environment of the fuel cell causes the deterioration and easy corrosion of the metallic BP. Hence researchers have focused on the investigation of alloy and composite materials with requisite characteristics for this application. The polymer matrix reinforced with carbon composite has received great interest as BP material due to their light weight, mechanical strength, and good conductivity. The superior properties of CNTs have made them good reinforcement materials as their addition increases electrical conductivity and the overall performance of BP. Daricik et al. [170] used MWCNT to modify carbon fibre/epoxy composite for BP material in PEMFC. The effect of different compositions of MWCNT (0.25–1.25 wt.%) reinforcement on the mechanical and electrical performance of CNT/CF/epoxy. The authors reported that CNT/CF/epoxy with 1.25 wt.% CNTs achieved an increased electrical conductivity of  $120 \text{ S}\cdot\text{cm}^{-2}$ . The inclusion of 1.25 wt.% CNTs were responsible for the increased flexural modulus and flexural strength of the composite BP. In another study, Ramirez-Herrera reported that the flexural strength, tensile strength, elastic modulus, and microhardness are all improved by 30%, 56%, 47% and 71% respectively when up to 20 wt.% of MWCNT is incorporated in polypropylene matrix via melt mixing technique. PP/MWCNT-20 wt.% nanocomposite showed increased electrochemical stability and very low deterioration when used as BP in PEMFC [171]. Polypropylene/milled carbon fibre/CNT (PP/MCF/CNT) composite BP fabricated via extrusion process was investigated by Radzuan et al. [172]. In the study, CNT was added to PP/MCF composite as a secondary filler and the effect of the secondary filler on the mechanical and electrical properties was examined. 25PP/70MCF/CNT5 composite gave the best BP characteristics with electrical conductivity of  $14.8 \text{ S}\cdot\text{cm}^{-1}$  flexural strength of 99.6 MPa and hardness of 83.4 and has potential application in PEMFC. The addition of 1 wt.% of CNT to polymer/graphite composite bipolar plate increased the through-plane thermal conductivity of the composite from 1 to  $13 \text{ W}\cdot(\text{mK})^{-1}$ . The increase was attributed to an increase in electron mobility caused by the presence of the CNT. While improved bending strength was due to the random orientation of MWCNT in the composite matrix [173]. Witpathomwong et al. [174] prepared polybenzoxazine (PBA) composited highly reinforced with graphene, graphite and MWCNT. The PBA/graphene/graphene/CNT composite has 84 wt.% of the total composite. The polymer composite containing 2 wt.% of CNTs achieved a thermal conductivity 44 times greater than the conductivity of a composite devoid of CNTs. Additionally, this composite demonstrated electrical conductivity of  $364 \text{ S}\cdot\text{cm}^{-1}$ , flexural strength of 41.5 MPa, and modulus of 49.7 GPa. In a certain study of the effect of CNT filler loading (1,2,3,...,10 wt.%) on the mechanical and electrical properties of PP/graphite/carbon black (PP/G/CB) composite as BP for PEMFC conducted by Bairan and coworkers [175]. It was confirmed that the increment in CNT content in the composite gave a synergistic effect that enhanced the flexural strength, electrical conductivity, hardness, and bulk density of the composite. However, at CNT composition  $>5$  wt.%, the mechanical properties of the composite began to deteriorate which was suggested to be caused by the poor bonding between the CNTs and other composite constituents. Also, with CNTs concentration above 6 wt.% a gradual decrease in electrical conductivity of the PP/G/CB/CNT composite was observed which was due to the critical agglomeration of CNTs. This finding was consistent with the research finding by Selamat et al. and Suherman et al. that affirm that excess incorporation of CNTs filler decreases the electrical conductivity of nanocomposites due to the aggregation of the CNTs particles [176,177]. 5 wt.% MWCNT filler content in PVDF/graphite/MWCNT composite BP achieved good flexural strength, good hydrophobicity, and high electrical conductivity. The MWCNT and graphite conductive fillers dispersed selectively in the polymer resin created a segregated conducting network in the polymer

matrix which resulted in the enhanced conductivity of the composite BP. The morphology and distribution of conductive filler (MWCNT and graphite) significantly affect the conductivity of the polymer composite BP. With the addition of different compositions of MWCNT (1, 3, 5, 7 wt.%) while maintaining the total filler composition of 40 wt.%, the MWCNT gradually covers the surface of the polymer resin and graphite flake thereby providing a conductive network which helps improve the conductivity of the composite. However, at 7 wt.% MWCNT loading the conductivity was adversely affected due to aggregation. The increase in mechanical properties of the composite was attributed to the high aspect ratio of the MWCNTs and the excellent network structure of MWCNTs which effectively transferred the load applied to the BP on the MWCNT. The increase in MWCNTs content increased the corrosion current density and decreased the corrosion resistance of PVDF/G/MWCNT composite BP in 0.5 M H<sub>2</sub>SO<sub>4</sub> acid at a temperature of 70 °C. The authors ascribe the reduction in corrosion resistance after addition of MWCNT to increased active sites on the BP composite surface, was responsible for minor side effects [178]. This was also in agreement with the assertion made by Oliveira et al. [179] in their study on the thermal and corrosion stability of polymer/graphite/MWCNT composite BP.

**Table 4.** Summary of mechanical and electrical properties of CNT composite BP and the US DOE requirement for BP.

BP composite material	Fabrication method	Flexural strength (MPa)	Shore hardness	Tensile (MPa)	Modulus (GPa)	Bulk density (g·cm <sup>-3</sup> )	Thermal conductivity W·(mK) <sup>-1</sup>	Electrical conductivity (S·cm <sup>-1</sup> )	Ref.
DOE BP target properties		>25	>50		<5	>10	>100		[175]
MCF65/PP30/CNT5	Extrusion	165.075	81.42		1.326		11.52		[172]
MCF70/PP25/CNT5	Extrusion	99.6205	83.4		1.378		14.77		[172]
PP/20MWCNT	Melt mixing	46.5		28.3					[171]
PP/15MWCNT/15CNF	Melt mixing	45.3		29.5					[171]
PBA/graphite/graphene/CNT-2 wt.%		41.5			49.7		21.3	364	[174]
35Phenolic resin/63graphite/2MWCNT	Compression moulding	56	57		14	1.82	50	145	[183]
PP/G/CB/CNT-6 wt.%	Compression moulding	27	81.5			1.64		158.32	[175]
PVDF/35G/%MWCNT	Structural design and Compression moulding	42						161.57	[178]

CNTs incorporated in a conducting polymer can also serve as a coating on metallic bipolar plates of PEMFC to enhance the corrosion resistance of the polymer used as a coating on the plate in an acidic environment. CNT increases the electrical conductivity of the coating film on

BP [167]. CNT/PTFE composite used as coating for SS304 BP achieved a reduction in the contact resistance between the BP and the MEA of the PEMFC and subsequently resulted in an increase in the output power [180]. Deyab reported an optimum corrosion inhibition efficiency and electrical conductivity of PANI coating on an aluminum bipolar plate by the addition of 0.8% CNT. CNT fillers in the polymer matrix improved the pore and charge transfer resistance of the coating [181]. The addition of CNT in composite polymer/graphite composite for BP increased the electrical conductivity by filling the pores in graphite and creating a more conductive path. In general CNT/polymer composite BP exhibit improve electrical and mechanical properties [182]. Table 4 shows the US Department of Energy (DOE) property requirement for PEMFC bipolar plates and other CNT-based composite BP.

In a typical PEMFC, the gas diffusion backing layer (GDBL) is in physical contact with the ribs of the bipolar plate. However, this interfacial contact is imperfect due to the porous nature of the GDBL, resulting in the generation of contact resistance at the interface between them [184]. Makharia et al. reported that the contact resistance between the GDBL and the bipolar plate contributes over 22% of the total electrical resistance of a typical PEMFC. The nanoporous structure of CNTs, along with their large surface area and electrical conductivity, has drawn the interest of researchers in utilizing the material as a cathodic interlayer in PEMFCs [185]. For instance, a comparative study conducted by Kim et al. in 2021 investigated CNT sheets fabricated via floating catalyst CVD and commercial carbon fiber employed as a functional microporous layer (MPL) in PEMFCs. The results showed that PEMFCs with CNT MPL (15  $\mu\text{m}$  thickness) exhibited a 50.9% increase in power density compared to those with commercial carbon black MPL [186]. In another study by Kwon and colleagues, MWCNTs were synthesized by direct spinning and deployed as a functional nanoporous layer to improve membrane electrode (ME) hydration and interfacial contact between the cathodic gas diffusion backing layer (GCBL) and the bipolar plate. The MEA with CNT interlayer delivered a power density of 364  $\text{mW}\cdot\text{cm}^{-2}$  at a potential of 0.7 and an increased pressure of 1.0 bar. Moreover, the MEA with CNT interlayer used in PEMFCs showed a 42% reduction in electrical resistance compared to conventional MEA due to improved interfacial contact and better hydration [184]. Holzapfel et al. prepared noble metal-free  $\text{Mo}_3\text{S}_{13}$ -NCNT as HER catalysts for use in PEM water electrolyzer. The chemical affinity between the nitrogen functional group of N-CNT and Mo enables their fabrication via self-assembly. The results showed that MEA using  $\text{Mo}_3\text{S}_{13}$ -NCNT catalyst loading of 3  $\text{mg}\cdot\text{cm}^{-2}$  exhibited a high current density of 4  $\text{A}\cdot\text{cm}^{-2}$  at a cell voltage of 2.36 V, which was the highest obtained for a noble metal-free cathode catalyst used for HER to date. Moreover, the MEA using  $\text{Mo}_3\text{S}_{13}$ -NCNT catalyst only degraded by 83  $\mu\text{V}\cdot\text{h}^{-1}$  after a 100 h stability test at 1  $\text{A}\cdot\text{cm}^{-2}$ . The overall electrochemical performance of the catalyst was attributed to the role of the nitrogen-functionalized CNT support in increasing porosity and electronic transport, thereby making more active sites available and resulting in improved electrochemical activity [187].

#### 4.6. CNT-based nanocomposite as anode material for fuel cell

A microbial fuel cell (MFC) is an eco-friendly and renewable type of proton exchange membrane fuel cell which utilizes a bio-electrical process (electroactive bacteria) to convert organic compounds or microbial metabolic energy into electricity [188]. However, the limitation in the commercialization of MFC is their low power density and low extracellular electron transfer (EET). Studies have shown that the anode material and its architecture strongly determine the adsorption of organic compounds and EET and in turn the performance of MFCs [189]. A high-performing anode is expected to show high corrosion resistance, biocompatibility, high electrical properties, and low electrical resistance [188].

The EET is determined by the interface between the anode and outer membrane cytochromes (OMCs). Commercial anodes of MFCs are usually made of carbon material (such as cloth, brush, paper). However, these carbon materials suffer from poor biocompatibility and surface reactivity [190]. CNTs have also been studied as an anode material for MFC because of their unique structural, high surface area and electrochemical properties which will enhance electrical energy generation in MFC [191]. Also, CNT has large aspect ratio and an ease for heteroatom doping which play a significant role in bacteria attachment and interfacial electron transport [192,193]. Studies have revealed that the use of functionalized CNT in MFC anode material resulted in an increased surface area to volume ratio which is desired anode property for higher power density in MFC. Ren et al. [194] examined the use of spin-spray layer-by-layer (SSLBL) CNT, vertically aligned CNT (V-CNT) and randomly aligned CNT (R-CNT)-based composite as anode materials. The report showed that all the surface-modified CNT exhibited improved volumetric power density and lower electrical resistance than bare gold anode electrodes. MFC cell with SSLBL-CNT-based anode achieved a maximum power density of  $3320 \text{ W}\cdot\text{m}^{-3}$ . The introduction of nitrogen-functionalized CNT into conducting polymers such as polyaniline (PANI) and polypyrrole (PPy) produced nanocomposites anode for MFC with a maximum power density of 202.3 and  $167.8 \text{ mW}\cdot\text{m}^{-2}$  for CNT/PANI and CNT/PPy composites respectively. The enhanced power generation capacity of the MFC was due to the synergistic effect of the electrical conductivity and high surface area of nitrogen-doped CNT and electrochemical properties of the conducting polymer. The nitrogen functional group in the composite improved the charge transport across the electrode [195]. The major challenge that affects the application of CNTs as anode materials is their cellular toxicity on electricigens growth which affect the generation of electric energy. Vertically grown CNT/polypyrrole on carbon fibre as MFC electrocatalyst anode delivered increased electrical energy with a power density of  $1876.62 \text{ mW}\cdot\text{m}^{-2}$  which is over 2.5 times higher than conventional carbon fibre anode. The high electrical energy generation of MFC made with VCNT/PPy composite anode was ascribed to the conductive network structure of VCNT on the CF which enhanced the mobility of electrons produced by electricigens to CFs surface. The presence of conducting PPy increases the biocompatibility of the anode and enhances the energy generation of the MFCs [191]. A combination of MWCNT and transition metal oxides such as  $\text{SnO}_2$ ,  $\text{MnO}_2$ , and  $\text{TiO}_2$  produce a composite anode material with improved surface wettability, biocompatible, enhanced kinetic activity, and high rate of electron transfer and power density [196–198]. Table 5 summarizes the power density of some CNT-based nanocomposite anode materials for MFC systems. Nickel based anode catalysts have been utilized in fuel cells such as SOFC, AFC and MFC due to their low cost, high thermal stability, high corrosion resistance and high electrocatalytic kinetic for ORR in a basic environment. However, in an operating environment of AFC, the Ni anode tends to disintegrate due to hydrogen-induced embrittlement of Ni, which drastically reduces the electrochemical performance of the fuel cells during operation. In addition, Ni surfaces suffer from partial passivation due to nickel oxide formation [199]. In hydrocarbon fuel cells, the Ni anode has high activity for carbon cracking [200]. Hence the modification of nickel catalysts with materials such as carbon nanotubes to improve long-term stability and increase resistance against hydrogen-induced embrittlement of Ni has been investigated. For instance, Mink et al. [201] synthesized vertically aligned forest functionalized MWCNT via the vapour-liquid-solid self-assembly method. The MWCNT was integrated into nickel silicide to form  $\text{NiSi}/\text{MWCNT}$  and the supported-on silicon substrate to produce an anode for MFC. MFC fabricated using the electrode delivered high current density and high-power generation. The presence of MWCNT increased chemical stability, biocompatibility, electrocatalytic activity and inhibit the decomposition of the anode. In another study, Zhang and coworkers compared the performance of the Ni/C electrode with a novel porous Ni/CNT loaded sponge (Ni/CNT@sponge) fabricated as an anode

electrode for urea microfluidic fuel cell. Ni/CNTs showed an improved electrical conductivity than Ni/C due to the presence of CNT. The Ni/CNT anode material exhibited increased surface area and homogeneous dispersion on the surface of the sponge after coating, this enhanced the fast penetration of the electrolyte ions and increased electrode reaction kinetics [202]. Tesfaye et al. [203] synthesized Ni-Co/MWCNT aerogel nanocomposite as an anode catalyst in urea fuel cells. The Ni-Co bimetal decorated on MWCNT aerogel delivered improved electrocatalytic activity with enhanced urea oxidation reaction. This was ascribed to MWCNT aerogel which provided a high surface area for the adsorption of the urea and 3D structure that allow a homogeneous distribution of Ni-Co nanoparticles. The Co metal decreased the start-up potential at which  $\text{Ni}^{2+}$  and OH transformed to  $\text{Ni}^{3+}$  OH and reduced the obstruction of catalyst by the products and controlled the oxygen evolution reaction. Gonzalez and co-workers [204] proposed Ni supported on CNT as a good electrocatalyst for ammonium oxidation reaction compared to Ni supported on carbon black. In their submission, CNT provided stability, higher surface area with enhanced surface oxidation which served as an anchor point for Ni nanoparticle attachment. The Ni/CNT catalyst also exhibited enhanced electrical conductivity. Ni@Pd/MWCNT composite electrocatalyst synthesized via two-step reduction process used as anode material in direct methanol fuel cell (DMFC). The composite electrocatalyst exhibited high catalytic activity toward the oxidation of methanol in alkaline electrolytes. Abrari et al. [205] developed Ni@Pd/MWCNT anode electrocatalyst prepared by a similar technique but using  $\text{Na}_3\text{C}_6\text{H}_5\text{O}_7$  and  $\text{NaBH}_4$  as stabilizer and reductant agents respectively. The Ni@Pd/MWCNT composite was used for formate oxidation reaction in a basic medium in a direct formate hydrogen peroxide fuel cell (DFHPFC). The metal nanoparticles (size range of 5–10 nm) were uniformly dispersed on MWCNT without agglomeration. Carbon cloth coated with NiO/CNT/PANI composite when employed as an anode material in MFC showed about 26.6% improvement in current density, 22% reduction in the internal resistance and 61.88% increase in the power density compared to conventional carbon cloth anode. The presence of CNT and PANI enhanced electron mobility from the bacteria cell to the anode electrode and was responsible for the improved electrochemical performance of the MFC. The high electric power generated was attributed to the strong hydrogen bond formation between the –COOH group in functionalized CNT and the N-group in the PANI which led to the overlapping of  $\pi-\pi^*$  electron clouds [206]. MWCNT supported by Ni/Cu/Mo trimetallic nanocomposite as an anode catalyst in direct methanol fuel cell (DMFC) exhibited high electroactivity for the methanol oxidation reaction [207]. Nazal and group reported that MWCNT/metal composite synthesized at different temperatures (900 and 1100 °C) revealed different levels of dispersibility of metal nanoparticles on MWCNTs. Microstructural analysis revealed that the composite synthesized at 1100 °C showed reduced agglomeration of metal nanoparticles, higher surface area and had smaller nanoparticle size (10–50 nm) compared to nanocomposite synthesized at 900 °C. An electrocatalyst made of Ni/Cu/Mo@MWCNTs composite showed better electroactivity and provided increased surface area for methanol oxidation reaction and methanol adsorption which consequently resulted in the reduction in charge transfer resistance at the electrode surface [207]. Integrated cobalt ferrite ( $\text{CoFe}_2\text{O}_4$ ) nanofiber into CNT developed by electrospinning, pyrolysis and in-situ hybrid technique and employed as MFC anode delivered excellent extracellular electron transfer boost.  $\text{CoFe}_2\text{O}_4/\text{CNT}$  composite showed power density of  $2290 \text{ mW}\cdot\text{m}^{-2}$  which is far higher than the power density of  $\text{CoFe}_2\text{O}_4$  and carbon cloth that were  $1458$  and  $497 \text{ mW}\cdot\text{m}^{-2}$  respectively. Additionally, the  $\text{CoFe}_2\text{O}_4/\text{CNTs}$  anode equipped MFCs displayed a coulombic efficiency of 30.5%, which was greater than those with  $\text{CoFe}_2\text{O}_4$  (25.9%) and the carbon cloth (CC) anodes (22.8%). The outstanding performance of the composite electrocatalyst was due to the synergistic effect of CNT and hollow  $\text{CoFe}_2\text{O}_4$ . The large surface area of the composite ensured enhanced bacterial loading and increased extracellular

electron transfer. The  $\text{CoFe}_2\text{O}_4$ /CNT composite anode exhibited high charge storage capacity and charge transfer rate which resulted in the improved electrochemical performance of MFC [208].

**Table 5.** CNT and CNT nanocomposite anode materials and their power density for Microbial fuel cell system.

MFC anode material	Anode loading ( $\text{mg}\cdot\text{cm}^{-2}$ )	Cathode	Cathode loading ( $\text{mg}\cdot\text{cm}^{-2}$ )	Power density ( $\text{mW}\cdot\text{m}^{-2}$ )	Ref.
CNT	1.2	40% Pt/C	0.705	145.3	[195]
PPY/CNT	0.63	40% Pt/C	1.01	167.8	[195]
PANI/CNT	0.86	40% Pt/C	1.01	202.3	[195]
Co $\text{Fe}_2\text{O}_4$ /CNT composite				2290	[208]
Nickel silicide (NiSi)/vertically aligned MWCNT		Carbon cloth		19.6	[201]
Ni/CNT@sponge		Pt/C		39000	[202]
Ni-Co/MWCNT aerogel nanocomposite				17.5	[203]
CNT		Gold foil		49	[209]
Graphite coated with $\text{MnO}_2$ (50)/MWCNT		Graphite		109.1	[197]
MWCNT		Graphite		18.1	[197]
CNT/PANI on macroporous graphite felt		Carbon cloth		257	[210]
3D carbon scaffold anodes from polyacrylonitrile		Air cathode		30.7	[211]
Glassy carbon/MWCNT/SnO <sub>2</sub> nanocomposite		Pt rod		1421	[196]
Spin spray layer by layer CNT		Air cathode		830	[194]
Vertically aligned CNT		Air cathode		270	[194]
Randomly aligned CNT		Air cathode		540	[194]
FeCo/NCNTs@CF		Graphite fiber		3040	[190]
Co/Ni@GC/NCNTs/CNFs	0.5	Pt ring	5.29	2100	[212]
Nitrophenyl-CNT	1.2	40 wt% Pt/C	0.9	393.8	[193]

Moreso, apart from the functionalization of CNTs via oxidation and doping with heteroatoms, nanostructured materials can be encapsulated into the hollow structure of CNTs. Compared to 0D, 2D, and 3D nanomaterials, CNTs have a unique one-dimensional structure of graphite sheets, offering numerous advantages. These include the ability to electronically interact with polarized electron density due to the curvature of  $\text{sp}^2$  carbons, the capability to interact electrically with d block components, very high mechanical strength, and the presence of inner nano-scale restricted regions. This inner restricted region has been utilized to encapsulate nanomaterials within CNTs, thereby achieving novel materials with improved mechanical stability and high-strength walls. Confined spaces not only facilitate catalytic reactions but also minimize the aggregation of nanomaterials, thereby increasing the shelf life of the catalyst. The technique used in the encapsulation of materials inside CNTs depends on the CNTs' diameter, viscosity, and surface tension of the solvents, as well as the boiling and melting points of the encapsulation materials. In fuel cell development, this confined space in CNTs has been exploited to fabricate catalyst materials with enhanced electrocatalytic activity and chemical stability [213]. For instance,  $\text{Ni}_3\text{Fe}$  nanoparticle encapsulated into CNT and grown on N-doped CNF via electrospinning exhibited improved electron transport capacity, gas diffusion, and showed high HER activity and chemical stability [119].

## 5. The challenges of CNT and its composites for fuel cell application and recommendations

CNTs, as nanoscale allotropes of carbon, consist of SWCNT or MWCNT cylindrical structures rolled from graphene sheets. They are highly desirable for use in various applications due to their remarkable one-dimensional electron conjugation, mechanical strength, and high chemical and thermal stability. However, despite these unique characteristics, the utilization and commercialization of CNTs have been greatly hindered by their hydrophobicity and insolubility in most solvents. This is attributed to the presence of strong van der Waals interactions, causing CNTs to naturally aggregate into bundles and clusters [33]. Additionally, the chemical interaction between pristine CNTs and other materials and compounds, such as polymers, is very poor. Furthermore, the various synthesis techniques for producing CNTs are accompanied by impurities such as carbon soot and residues from the catalyst employed, which also limit the application of CNTs. Research has shown that surface modification of CNTs using surfactants can enhance hydrophilicity and solubility of CNTs in many solvents, as well as increase the chemical interaction between CNTs and other compounds and molecules. The production of CNT/metal oxide (CNT/MO) nanocomposites involves three steps: functionalization, adsorption of metal nanoparticles on CNTs, and heat treatment [71,196]. However, this synthesis process is complex, alters the electronic structure of the composite, and is not environmentally friendly [72]. The authors recommend a one-step or two-step solvothermal process that would not involve the chemical degradation of composite constituents and would not pose chemical hazards to the environment. Additionally, metal nanoparticle decoration and functionalization with polymer would simplify the creation of new nanomaterials and nanodevices. The incorporation of metal oxide as a spacer in Pt/CNT will also increase the poison tolerance and durability of the catalyst due to the strong interaction between the noble metal, carbon nanotubes, and metal oxides [214]. The design, fabrication, and commercialization of fuel cells as an eco-friendly and efficient energy source have received considerable attention and found applications in portable electronics, automobiles, and stationary power generation systems. However, the high cost of fuel cells, greatly contributed by the cost of Pt noble metal catalyst, has limited the commercial development of this energy conversion system. Besides cost, Pt dissolves and agglomerates under harsh operating conditions, exhibiting low activity and instability [215,216]. Hence, researchers have considered CNTs, and their composites as good catalyst supports that will not only reduce the amount of Pt used in fuel cell production but also exhibit high electroactivity, thermal stability, and chemical performance. From the literature, many researchers have reported that incorporating functionalized CNTs will enhance their chemical compatibility and dispersion of other materials. The use of CNTs as reinforcement in the development of bipolar plates will result in lightweight materials with improved mechanical strength compared to the use of graphite, metal powder, and carbon fiber, making them excellent materials for fuel cell applications. CNT loading in polymer-based composites utilized as bipolar plates in PEMFCs showed a synergistic effect, improving electrical conductivity, bulk density, hardness, and flexural strength of the composite. However, the application of functionalized CNT composites in fuel cells has still been challenged with agglomeration, with poorly dispersed CNTs in the matrix material due to the high surface energy of the nanotube, thereby preventing the creation of a conductive path that would otherwise lead to improved conductivity [170,175]. However, functionalized CNT composite application in fuel cells has still been challenged with agglomeration with poorly dispersed CNT in the matrix material due to the high surface energy of the nanotube, thereby preventing the creation of a conductive path that would otherwise lead to improved conductivity. Based on the reviews carried out and the challenges observed, the authors recommend that great attention should be given to the development of functionalized CNT composites with conducting polymer via the solution melt technique. Melt

mixing with an internal mixer will drastically reduce the agglomeration of CNTs in the polymer matrix. Proper dispersion of metal, bimetallic, and trimetallic alloy nanoparticles on the CNT matrix can be employed as one of the prerequisites for obtaining high electrocatalytic activity for oxidation reactions in fuel cells. Wet impregnation and subsequent careful heat treatment procedures can be used to achieve this. The authors also recommend the exploitation of the confined space in CNTs and strategic encapsulation of different nanoparticles into this restricted space. This encapsulation into CNTs confined space is expected to drastically reduce agglomeration, increase stability, and enhance electrocatalytic performance of CNT composite-based electrodes.

Furthermore, the commercial utilization of CNT composite especially for application in energy storage and conversion system demands a careful study into the surface interaction between the CNT and the reinforcing constituents in order to achieve optimum performance. Careful optimization of the side wall and end wall functionalization of carbon nanotube with oxidizing agents such as acids must be done to avoid the introduction of excessive defect and over-oxidation of CNT which will result in the deterioration of the mechanical and electrical properties of CNT composite. It is also paramount to consider other synthesis techniques, such as reduction expansion synthesis, that can deliver low internal resistance, high ion and electron transport, a large contact surface area, ensure proper homogenization, and reduce agglomeration.

## 6. Summary

Fuel cells are considered one of the most promising technologies to address prevalent energy issues and environmental concerns due to their characteristics, such as excellent energy conversion and reduced pollutant emissions. This review article presents CNTs, their functionalization, and CNT nanocomposites, focusing on their applications in fuel cells. Functionalization enables the creation of active sites that promote the dispersion of metal nanoparticles on the functionalized CNTs, making it a useful method for enhancing both the interaction and reactivity of CNTs. The development of the novel outstanding physical, electrical, and mechanical properties of CNTs has drawn significant interest from researchers exploring their potential applications in energy storage and conversion systems. The use of CNT composites as electrocatalyst support, MEAs, and bipolar plates was reviewed, with emphasis on the effect of CNTs on the mechanical, corrosion, and electrochemical performance of fuel cells. This review study highlights the significance of CNT composite support for Pt and Ni catalyst electrodes and the influence of CNTs in enhancing the catalytic activity, stability, and overall performance of fuel cells. Furthermore, the use of CNTs and CNT composites has significantly reduced the utilization of Pt and noble metals, contributing to the cost reduction of fuel cells. CNTs and their composites supported on metallic nanoparticles have demonstrated high electroactivity and mechanical properties. Studies on the remarkable potential of CNTs as reinforcements in polymer composites reveal that these composites not only exhibit distinctive intrinsic features, including mechanical, electrical, and thermal capabilities but also cooperative or synergetic effects. CNTs incorporated into conducting polymers can be used as a coating on bipolar plates of PEMFCs to enhance corrosion resistance in acidic environments. However, increased CNT content in the composite may lead to agglomeration, resulting in degradation of these outstanding composite properties. Therefore, there is a need to optimize the amount of CNT in the composite material to deliver optimum electrocatalyst performance. Additionally, there remains a gap in the literature, and further research into the microscopic transport mechanisms of CNTs is still required, necessitating highly capable molecular dynamic simulations.

## Use of AI tools declaration

The authors declare they have not used Artificial Intelligence (AI) tools in the creation of this article.

## Conflict of interest

The authors declare no conflict of interest.

## References

1. Fan L, Tu Z, Chan S (2021) Recent development of hydrogen and fuel cell technologies: A review. *Energy Rep* 7: 8421–8446. <https://doi.org/10.1016/j.egyr.2021.08.003>
2. Wu Z, Dang D, Tian X (2019) Designing robust support for Pt alloy nanoframes with durable oxygen reduction reaction activity. *ACS Appl Mater Interfaces* 11: 9117–9124. <https://doi.org/10.1021/acsmami.8b21459>
3. Su H, Hu Y (2021) Recent advances in graphene-based materials for fuel cell applications. *Energy Sci Eng* 9: 958–983. <https://doi.org/10.1002/ese3.833>
4. Hou J, Yang M, Ke C, et al. (2020) Platinum-group-metal catalysts for proton exchange membrane fuel cells: From catalyst design to electrode structure optimization. *EnergyChem* 2:100023. <https://doi.org/10.1016/j.enchem.2019.100023>
5. Kanninen P, Eriksson B, Davodi F, et al. (2020) Carbon corrosion properties and performance of multi-walled carbon nanotube support with and without nitrogen-functionalization in fuel cell electrodes. *Electrochim Acta* 332: 135384. <https://doi.org/10.1016/j.electacta.2019.135384>
6. Li X, Li Y, Xie S, et al. (2022) Zinc-based energy storage with functionalized carbon nanotube/polyaniline nanocomposite cathodes. *Chem Eng J* 427: 131799. <https://doi.org/10.1016/j.cej.2021.131799>
7. Roy R, Soundiraraju B, Thomas D, et al. (2017) New insights into the spectral, thermal and morphological analysis of time dependent structural changes during open end functionalization of single walled carbon nanotubes. *New J Chem* 20: 12159–12171. <https://doi.org/10.1039/C7NJ01843F>
8. Ates M, Eker A, Eker B (2017) Carbon nanotube-based nanocomposites and their applications. *J Adhes Sci Technol* 31: 1977–1997. <https://doi.org/10.1080/01694243.2017.1295625>
9. Iijima S (1991) Helical microtubules of graphitic carbon. *Nature* 354: 56–58. <https://www.nature.com/articles/354056a0/metrics>
10. Bilalis P, Katsigianopoulos D, Avgeropoulos A, et al. (2014) Non-covalent functionalization of carbon nanotubes with polymers. *RSC Adv* 4: 2911–2934. <http://doi.org/10.1039/C3RA44906H>
11. Soni S, Thomas B, Kar VA (2020) A comprehensive review on CNTs and CNT-reinforced composites: Syntheses, characteristics and applications. *Mater Today Commun* 25: 101546. <https://doi.org/10.1016/j.mtcomm.2020.101546>
12. Chen J, Liu B, Gao X, et al. (2018) Review of the interfacial characteristics of polymer nanocomposites containing carbon nanotubes. *RSC Adv* 8: 28048–28085. <http://doi.org/10.1039/C8RA04205E>
13. Verma B, Sewani H, Balomajumder C (2020) Synthesis of carbon nanotubes via chemical vapor deposition: An advanced application in the management of electroplating effluent. *Environ Sci Pollut Res* 27: 14007–14018. <https://doi.org/10.1007/s11356-020-08002-0>

14. Krishnamurthy G, Namitha R, Agarwal S (2014) Synthesis of carbon nanotubes and carbon spheres and study of their hydrogen storage property by electrochemical method. *Procedia Mater Sci* 5:1056–1065. <https://doi.org/10.1016/j.mspro.2014.07.397>
15. Han S, Yang J, Li X, et al. (2020) Flame synthesis of super hydrophilic carbon nanotubes/Ni foam decorated with  $\text{Fe}_2\text{O}_3$  nanoparticles for water purification via solar steam generation. *ACS Appl Mater Interfaces* 12: 13229–13238. <https://doi.org/10.1021/acsami.0c00606>
16. Toleukhanuly Y, Kuttybaevna K, Muratbekovna K, et al. (2020) Synthesis of carbon nanotubes by the electric arc-discharge method. *Series Chem Technol* 5: 126–133. <http://doi.org/10.32014/2020.2518-1491.89>
17. Cheng Y, Zhao S, Johannessen B, et al. (2018) Atomically dispersed transition metals on carbon nanotubes with ultrahigh loading for selective electrochemical carbon dioxide reduction. *Adv Mater* 13: 1706287. <https://doi.org/10.1002/adma.201706287>
18. Ismail R, Mousa A, Amin M (2018) Synthesis of hybrid  $\text{Au}@\text{PbI}_2$  core-shell nanoparticles by pulsed laser ablation in ethanol. *Mater Res Express* 5: 115024. <http://doi.org/10.1088/2053-1591/aadf1b>
19. Alheshibri M, Elsayed K, Haladu S, et al. (2022) Synthesis of Ag nanoparticles-decorated on CNTs/TiO<sub>2</sub> nanocomposite as efficient photocatalysts via nanosecond pulsed laser ablation. *Opt Laser Technol* 155: 108443. <https://doi.org/10.1016/j.optlastec.2022.108443>
20. Mubarak N, Abdullah E, Jayakumar N, et al. (2014) An overview on methods for the production of carbon nanotubes. *J Ind Eng Chem* 20: 1186–1197. <https://doi.org/10.1016/j.jiec.2013.09.001>
21. Ismail R, Mohsin M, Ali A, et al. (2020) Preparation and characterization of carbon nanotubes by pulsed laser ablation in water for optoelectronic application. *Physica E Low Dimens Syst Nanostruct* 119: 113997. <https://doi.org/10.1016/j.physe.2020.113997>
22. Eatemadi A, Daraee H, Karimkhanloo H, et al. (2014) Carbon nanotubes: Properties, synthesis, purification, and medical applications. *Nanoscale Res Lett* 9: 393. <http://www.nanoscalereslett.com/content/9/1/393>
23. Joselevich E, Dai H, Liu J, et al. (2008) Carbon nanotube synthesis and organization, In: Jorio A, Dresselhaus G, Dresselhaus M, *Carbon Nanotubes: Advanced Topics in the Synthesis, Structure, Properties and Applications*, Berlin: Springer. [http://doi.org/10.1007/978-3-540-72865-8\\_4](http://doi.org/10.1007/978-3-540-72865-8_4)
24. Ganguly D, Sundara R, Ramanujam K (2018) Chemical vapor deposition-grown nickel-encapsulated N-doped carbon nanotubes as a highly active oxygen reduction reaction catalyst without direct metal–nitrogen coordination. *ACS Omega* 3: 13609–13620. <https://doi.org/10.1021/acsomega.8b01565>
25. Pandey P, Dahiya M (2016) Carbon nanotubes: Types, methods of preparation and applications. *Int J Pharm Sci Res* 4: 15–21.
26. Ahmad M, Silva SR (2020) Low temperature growth of carbon nanotubes—A review. *Carbon* 158: 24–44. <https://doi.org/10.1016/j.carbon.2019.11.061>
27. Halonen N, Sapi A, Nagy J, et al. (2011) Low-temperature growth of multi-walled carbon nanotubes by thermal CVD. *Phys Status Solidi B* 248: 2500–2503. <https://doi.org/10.1002/pssb.201100137>
28. Simionescu O, Brîncoveanu O, Romanițan C, et al. (2022) Step-by-step development of vertically aligned carbon nanotubes by plasma-enhanced chemical vapor deposition. *Coatings* 12: 943. <https://doi.org/10.3390/coatings12070943>
29. Shoukat R, Khan M (2022) Carbon nanotubes/nanofibers (CNTs/CNFs): A review on state of the art synthesis methods. *Microsyst Technol* 28: 885–890. <https://doi.org/10.1007/s00542-022-05263-2>

30. Shoukat R, Muhammad I (2021) Carbon nanotubes: A review on properties, synthesis methods and applications in micro and nanotechnology. *Microsyst Technol* 27: 4183–4192. <https://doi.org/10.1007/s00542-021-05211-6>
31. Jagadeesan A, Thangavelu K, Dhananjeyan V (2020) Carbon nanotubes: Synthesis, properties and applications, In: Pham P, Goel P, Kumar S, et al. *21st Century Surface Science-a Handbook*, London: Intech Open. <http://dx.doi.org/10.5772/intechopen.92995>
32. Punetha V, Rana S, Yoo H, et al. (2017) Functionalization of carbon nanomaterials for advanced polymer nanocomposites: A comparison study between CNT and graphene. *Prog Polym Sci* 67: 1–47. <https://doi.org/10.1016/j.progpolymsci.2016.12.010>
33. Luais E, Thobie-Gautier C, Tailleur A, et al. (2010) Preparation and modification of carbon nanotubes electrodes by cold plasmas processes toward the preparation of amperometric biosensors. *Electrochim Acta* 55: 7916–7922. <https://doi.org/10.1016/j.electacta.2010.02.070>
34. Steffen T, Fontana L, Hammer P, et al. (2019) Carbon nanotube plasma functionalization: The role of carbon nanotube/maleic anhydride solid premix. *Appl Surf Sci* 491: 405–410. <https://doi.org/10.1016/j.apsusc.2019.06.176>
35. Yang N, Chen X, Ren T, et al. (2015) Carbon nanotube based biosensors. *Sensor Actuat B-Chem* 207: 690–715. <https://doi.org/10.1016/j.snb.2014.10.040>
36. Ribeiro B, Botelho E, Costa M, et al. (2017) Carbon nanotube buckypaper reinforced polymer composites: A review. *Polímeros* 27: 247–255. <https://doi.org/10.1590/0104-1428.03916>
37. Janudin N, Abdullah N, Yunus W, et al. (2019) Carbon nanofibers functionalized with amide group for ammonia gas detection. *AIP Conf Proc* 2068: 020061. <https://doi.org/10.1063/1.5089360>
38. Karousis N, Tagmatarchis N, Tasis D (2010) Current progress on the chemical modification of carbon nanotubes. *Chem Rev* 110: 5366–5397. <https://doi.org/10.1021/cr100018g>
39. Zhang J, Zou H, Qing Q, et al. (2003) Effect of chemical oxidation on the structure of single-walled carbon nanotubes. *J Phys Chem B* 107: 3712–3718. <https://doi.org/10.1021/jp027500u>
40. Chen J, Hamon M, Hu H, et al. (1998) Solution properties of single-walled carbon nanotubes. *Science* 282: 95–98. <http://doi.org/10.1126/science.282.5386.95>
41. Goyanes S, Rubiolo G, Salazar A, et al. (2007) Carboxylation treatment of multiwalled carbon nanotubes monitored by infrared and ultraviolet spectroscopies and scanning probe microscopy. *Diam Relat Mater* 16: 412–417. <https://doi.org/10.1016/j.diamond.2006.08.021>
42. Malikov E, Akperov O, Muradov M, et al. (2014) Oxidation of multiwalled carbon nanotubes using different oxidation agents like nitric acid and potassium permanganate. *News Baku University* 4: 49–59.
43. Abdelkader V, Scelfo S, García-Gallarín C, et al. (2013) Carbon tetrachloride cold plasma for extensive chlorination of carbon nanotubes. *J Phys Chem C* 117: 16677–16685. <https://doi.org/10.1021/jp404390h>
44. Zhou Z, Orcutt E, Anderson H, et al. (2019) Hydrogen surface modification of a carbon nanotube catalyst for the improvement of ethane oxidative dehydrogenation. *Carbon* 152: 924–931. <https://doi.org/10.1016/j.carbon.2019.06.076>
45. Adamska M, Narkiewicz U (2017) Fluorination of carbon nanotubes—A review. *J Fluorine Chem* 200: 179–189. <https://doi.org/10.1016/j.jfluchem.2017.06.018>
46. Kim J, Jeong E, Lee Y (2016) Characteristics of fluorinated CNTs added carbon foams. *Appl Surf Sci* 360: 1009–1015. <https://doi.org/10.1016/j.apsusc.2015.11.111>

47. Norizan M, Moklis M, Demon S, et al. (2020) Carbon nanotubes: Functionalisation and their application in chemical sensors. *RSC Adv* 10: 43704–43732. <http://doi.org/10.1039/D0RA09438B>

48. Sabet S, Mahfuz H, Terentis A, et al. (2018) Effects of POSS functionalization of carbon nanotubes on microstructure and thermomechanical behavior of carbon nanotube/polymer nanocomposites. *J Mater Sci* 53: 8963–8977. <https://doi.org/10.1007/s10853-018-2182-y>

49. Wang C, Wu H, Qu F, et al. (2016) Preparation and properties of polyvinyl chloride ultrafiltration membranes blended with functionalized multi-walled carbon nanotubes and MWCNTs/Fe<sub>3</sub>O<sub>4</sub> hybrids. *J Appl Polym Sci* 133: 43417. <https://doi.org/10.1002/app.43417>

50. Vatanpour V, Madaeni S, Moradian R, et al. (2012) Novel antibifouling nanofiltration polyethersulfone membrane fabricated from embedding TiO<sub>2</sub> coated multiwalled carbon nanotubes. *Sep Purif Technol* 90: 69–82. <https://doi.org/10.1016/j.seppur.2012.02.014>

51. Zhu C, Zhang M, Qiao Y, et al. (2010) Fe<sub>3</sub>O<sub>4</sub>/TiO<sub>2</sub> core/shell nanotubes: Synthesis and magnetic and electromagnetic wave absorption characteristics. *J Phys Chem C* 114: 16229–16235. <https://doi.org/10.1021/jp104445m>

52. Fujigaya T, Nakashima N (2015) Non-covalent polymer wrapping of carbon nanotubes and the role of wrapped polymers as functional dispersants. *Sci Technol Adv Mater* 16: 024802. <http://doi.org/10.1088/1468-6996/16/2/024802>

53. Dai J, Fernandes R, Regev O, et al. (2018) Dispersing carbon nanotubes in water with amphiphiles: Dispersant adsorption, kinetics, and bundle size distribution as defining factors. *J Phys Chem C* 122: 24386–24393. <https://doi.org/10.1021/acs.jpcc.8b06542>

54. Wang X, Bai L, Kong S, et al. (2019) Star-shaped supramolecular ionic liquid crystals based on pyridinium salts. *Liq Cryst* 46: 512–522. <https://doi.org/10.1080/02678292.2018.1512166>

55. Manilo MV, Lebovka N, Barany S (2017) Combined effect of cetyltrimethylammonium bromide and laponite platelets on colloidal stability of carbon nanotubes in aqueous suspensions. *J Mol Liq* 235: 104–110. <https://doi.org/10.1016/j.molliq.2017.01.090>

56. Kharisov B, Kharissova O, Dimas A (2016) The dispersion, solubilization and stabilization in “solution” of single-walled carbon nanotubes. *RSC Adv* 6: 68760–68787. <http://doi.org/10.1039/C6RA13187E>

57. Zeng X, Yang D, Liu H, et al. (2018) Detecting and tuning the interactions between surfactants and carbon nanotubes for their high-efficiency structure separation. *Adv Mater Interfaces* 5: 1700727. <https://doi.org/10.1002/admi.201700727>

58. Park M, Park J, Lee J, et al. (2018) Scaling of binding affinities and cooperativities of surfactants on carbon nanotubes. *Carbon* 139: 427–436. <https://doi.org/10.1016/j.carbon.2018.07.003>

59. Berber M, Hafez I, Mustafa M (2019) Surface functionalization of carbon nanotubes for energy applications, In: Saleh H, Mohamed El-Sheikh S, *Perspective of Carbon Nanotubes*, London: Intech Open. <https://dx.doi.org/10.5772/intechopen.84479>

60. Goutam P, Singh D, Giri P, et al. (2011) Enhancing the photostability of poly(3-hexylthiophene) by preparing composites with multiwalled carbon nanotubes. *J Phys Chem B* 115: 919–924. <https://doi.org/10.1021/jp109900m>

61. Li M, Xu P, Yang J, et al. (2011) Synthesis of pyrene-substituted poly(3-hexylthiophene) via postpolymerization and its noncovalent interactions with single-walled carbon nanotubes. *J Phys Chem C* 115: 4584–4593. <https://doi.org/10.1021/jp112330n>

62. Abu-Abdeen M, Ayesh A, Al Jaafari A (2012) Physical characterizations of semi-conducting conjugated polymer-CNTs nanocomposites. *J Polym Res* 19: 1–9. <http://doi.org/10.1007/s10965-012-9839-z>

63. Hong JH, Park DW, Shim SE (2010) A review on thermal conductivity of polymer composites using carbon-based fillers: Carbon nanotubes and carbon fibers. *Carbon Lett* 11: 347–356. <https://doi.org/10.5714/CL.2010.11.4.347>

64. Hong SK, Kim D, Lee S, et al. (2015) Enhanced thermal and mechanical properties of carbon nanotube composites through the use of functionalized CNT-reactive polymer linkages and three-roll milling. *Compos Part A-Appl S* 77: 142–146. <https://doi.org/10.1016/j.compositesa.2015.05.035>

65. Dang Z, Wang L, Yin Y, et al. (2007) Giant dielectric permittivities in functionalized carbon-nanotube/electroactive-polymer nanocomposites. *Adv Mater* 19: 852–857. <https://doi.org/10.1002/adma.200600703>

66. Kharisov B, Kharissova O, Ortiz Mendez U, et al. (2016) Decoration of carbon nanotubes with metal nanoparticles: Recent trends. *Synth React Inorg M* 46: 55–76. <https://doi.org/10.1080/15533174.2014.900635>

67. Roy RE, Vijayalakshmi K, Bhuvaneswari S, et al. (2019) Influence of process conditions and effect of functionalization in inducing time dependent polymorphic states in single walled carbon nanotube incorporated poly(vinylidene fluoride). *SN Appl Sci* 1: 1–15. <https://doi.org/10.1007/s42452-019-0862-0>

68. Shirvanimoghaddam K, Abolhasani M, Polisetti B, et al. (2018) Periodical patterning of a fully tailored nanocarbon on CNT for fabrication of thermoplastic composites. *Compos Part A-Appl S* 107: 304–314. <https://doi.org/10.1016/j.compositesa.2018.01.015>

69. Zadehnazari A, Takassi MA (2016) Synthesis of modified multi-walled carbon nanotube poly(benzimidazole-imide) composites: Assessment of morphological and thermo-mechanical properties. *Compos Interface* 23: 909–924. <https://doi.org/10.1080/09276440.2016.1180500>

70. Soldano C (2015) Hybrid metal-based carbon nanotubes: Novel platform for multifunctional applications. *Prog Mater Sci* 69: 183–212. <https://doi.org/10.1016/j.pmatsci.2014.11.001>

71. Abbas S, Ahmad N, Rana U, et al. (2016) High rate capability and long cycle stability of  $\text{Cr}_2\text{O}_3$  anode with CNTs for lithium ion batteries. *Electrochim Acta* 212: 260–269. <https://doi.org/10.1016/j.electacta.2016.06.156>

72. Cheng Y, Huang J, Qi H, et al. (2017) Adjusting the chemical bonding of  $\text{SnO}_2@\text{CNT}$  composite for enhanced conversion reaction kinetics. *Small* 13: 1700656. <https://doi.org/10.1002/smll.201700656>

73. Long H, Guo C, Wei G, et al. (2019) Facile synthesis of various carbon nanotube/metal oxide nanocomposites with high quality. *Vacuum* 166: 147–150. <https://doi.org/10.1016/j.vacuum.2019.05.002>

74. Ling B, Chen A, Liu W, et al. (2018) Simply and rapidly synthesized composites of  $\text{MnO}_2$  nanosheets anchoring on carbon nanotubes as efficient sulfur hosts for Li-S batteries. *Mater Lett* 218: 321–324. <https://doi.org/10.1016/j.matlet.2018.02.030>

75. Zhou J, Song H, Ma L, et al. (2011) Magnetite/graphene nanosheet composites: Interfacial interaction and its impact on the durable high-rate performance in lithium-ion batteries. *RSC Adv* 1: 782–791. <https://doi.org/10.1039/C1RA00402F>

76. Liu X, Li S, Akinwolemiwa B, et al. (2021) Low-crystalline transition metal oxide/hydroxide on MWCNT by Fenton-reaction-inspired green synthesis for lithium ion battery and OER electrocatalysis. *Electrochim Acta* 387: 138559. <https://doi.org/10.1016/j.electacta.2021.138559>

77. Sigwadi R, Dhlamini M, Mokrani T, et al. (2019) Enhancing the mechanical properties of zirconia/Nafion® nanocomposite membrane through carbon nanotubes for fuel cell application. *Heliyon* 5: 02112. <https://doi.org/10.1016/j.heliyon.2019.e02112>

78. Mallakpour S, Khadem E (2016) Carbon nanotube–metal oxide nanocomposites: Fabrication, properties and applications. *Chem Eng J* 302: 344–367. <https://doi.org/10.1016/j.cej.2016.05.038>

79. Amina Sarfraz, Asif Hassan R, Mojtaba M, et al. (2022) Electrode materials for fuel cells, In: Abdul-Ghani O, *Encyclopedia of Smart Materials*, Oxford: Elsevier, 2: 341–356. <http://doi.org/10.1016/B978-0-12-803581-8.11742-4>

80. Peera S, Koutavarapu R, Akula S, et al. (2021) Carbon nanofibers as potential catalyst support for fuel cell cathodes: A review. *Energ Fuel* 35: 11761–11799. <https://doi.org/10.1021/acs.energyfuels.1c01439>

81. Ehte E (2016) Study of two-phase flow pressure drop characteristics in proton exchange membrane (PEM) fuel cell flow channels of different geometries. Available from: <https://www.proquest.com/openview/ee37bf13dafcc44451cc66df52b78e99/1?cbl=18750&pq-origsite=gscholar&parentSessionId=CuRlwPj0ED%2FiNBD58cDez%2B%2FLvT09U2ao4FrBLrP5NcA%3D>.

82. Penner S (1995) Report of the DOE advanced fuel-cell commercialization working group. Available from: <https://www.osti.gov/servlets/purl/810985>.

83. Larminie J (2003) *Fuel Cell Systems Explained*, 2 Eds., UK: Wiley, 2: 207–225. Available from: [https://sv.20file.org/up1/482\\_0.pdf](https://sv.20file.org/up1/482_0.pdf).

84. Williams M, Strakey J, Sudoval W (2006) US DOE fossil energy fuel cells program. *J Power Sources* 159: 1241–1247. <https://doi.org/10.1016/j.jpowsour.2005.12.085>

85. Staffell I, Green R, Kendall K (2008) Cost targets for domestic fuel cell CHP. *J Power Sources* 181: 339–349. <https://doi.org/10.1016/j.jpowsour.2007.11.068>

86. AL-bonsrulah H, Alshukri M, Mikhael L, et al. (2021) Design and simulation studies of hybrid power systems based on photovoltaic, wind, electrolyzer, and pem fuel cells. *Energies* 14: 2643. <https://doi.org/10.3390/en14092643>

87. Antolini E (2016) Structural parameters of supported fuel cell catalysts: The effect of particle size, inter-particle distance and metal loading on catalytic activity and fuel cell performance. *Appl Catal B-Environ* 181: 298–313. <https://doi.org/10.1016/j.apcatb.2015.08.007>

88. Islam M, Mansoor B, Kollath V, et al. (2022) Designing fuel cell catalyst support for superior catalytic activity and low mass-transport resistance. *Nat Commun* 13: 6157. <https://doi.org/10.1038/s41467-022-33892-8>

89. Akbari E, Buntat Z (2017) Benefits of using carbon nanotubes in fuel cells: A review. *Int J Energy Res* 41: 92–102. <https://doi.org/10.1002/er.3600>

90. Mu Y, Liang H, Hu J, et al. (2005) Controllable Pt nanoparticle deposition on carbon nanotubes as an anode catalyst for direct methanol fuel cells. *J Phys Chem B* 109: 22212–22216. <https://doi.org/10.1021/jp0555448>

91. Hyeon T, Han S, Sung YE, et al. (2003) High-performance direct methanol fuel cell electrodes using solid-phase-synthesized carbon nanocoils. *Angew Chem Int Ed* 42: 4352–4356. <https://doi.org/10.1002/anie.200250856>

92. Samad S, Loh KS, Wong WY, et al. (2018) Carbon and non-carbon support materials for platinum-based catalysts in fuel cells. *Int J Hydrogen Energy* 43: 7823–7854. <https://doi.org/10.1016/j.ijhydene.2018.02.154>

93. Devrim Y, Arica ED, Albostan A (2018) Graphene based catalyst supports for high temperature PEM fuel cell application. *Int J Hydrogen Energy* 43: 11820–11829. <https://doi.org/10.1016/j.ijhydene.2018.03.047>

94. Zhang N, Li L, Chu Y, et al. (2019) High Pt utilization efficiency of electrocatalysts for oxygen reduction reaction in alkaline media. *Catal Today* 332: 101–108. <https://doi.org/10.1016/j.cattod.2018.07.018>

95. Mu X, Xu Z, Ma Y, et al. (2017) Graphene-carbon nanofiber hybrid supported Pt nanoparticles with enhanced catalytic performance for methanol oxidation and oxygen reduction. *Electrochim Acta* 253: 171–177. <https://doi.org/10.1016/j.electacta.2017.09.029>

96. Wang Y, Li G, Jin J, et al. (2017) Hollow porous carbon nanofibers as novel support for platinum-based oxygen reduction reaction electrocatalysts. *Int J Hydrogen Energy* 42: 5938–5947. <https://doi.org/10.1016/j.ijhydene.2017.02.012>

97. Tong X, Zhang J, Zhang G, et al. (2017) Ultrathin carbon-coated Pt/carbon nanotubes: A highly durable electrocatalyst for oxygen reduction. *Chem Mater* 29: 9579–9587. <https://doi.org/10.1021/acs.chemmater.7b04221>

98. Wang YJ, Fang B, Li H, et al. (2016) Progress in modified carbon support materials for Pt and Pt-alloy cathode catalysts in polymer electrolyte membrane fuel cells. *Prog Mater Sci* 82: 445–498. <https://doi.org/10.1016/j.pmatsci.2016.06.002>

99. Sui S, Wang X, Zhou X, et al. (2017) A comprehensive review of Pt electrocatalysts for the oxygen reduction reaction: Nanostructure, activity, mechanism and carbon support in PEM fuel cells. *J Mater Chem A* 5: 1808–1825. <https://doi.org/10.1039/C6TA08580F>

100. Fan L, Zhao J, Luo X, et al. (2022) Comparison of the performance and degradation mechanism of PEMFC with Pt/C and Pt black catalyst. *Int J Hydrogen Energy* 47: 5418–5428. <https://doi.org/10.1016/j.ijhydene.2021.11.135>

101. Li Y, Li J, Wang YG, et al. (2021) Carbon corrosion mechanism on nitrogen-doped carbon support—A density functional theory study. *Int J Hydrogen Energy* 46: 13273–13282. <https://doi.org/10.1016/j.ijhydene.2021.01.148>

102. Borup RL, Kusoglu A, Neyerlin KC, et al. (2020) Recent developments in catalyst-related PEM fuel cell durability. *Curr Opin Electroche* 21: 192–200. <https://doi.org/10.1016/j.coelec.2020.02.007>

103. Hu Z, Xu L, Gan Q, et al. (2021) Carbon corrosion induced fuel cell accelerated degradation warning: From mechanism to diagnosis. *Electrochim Acta* 389: 138627. <https://doi.org/10.1016/j.electacta.2021.138627>

104. Sabawa J, Bandarenka A (2021) Investigation of degradation mechanisms in PEM fuel cells caused by low-temperature cycles. *Int J Hydrogen Energy* 46: 15951–15964. <https://doi.org/10.1016/j.ijhydene.2021.02.088>

105. Zheng Z, Yang F, Lin C, et al. (2020) Design of gradient cathode catalyst layer (CCL) structure for mitigating Pt degradation in proton exchange membrane fuel cells (PEMFCs) using mathematical method. *J Power Sources* 451: 227729. <https://doi.org/10.1016/j.jpowsour.2020.227729>

106. Sun X, Yu H, Zhou L, et al. (2020) Influence of platinum dispersity on oxygen transport resistance and performance in PEMFC. *Electrochim Acta* 332: 135474. <https://doi.org/10.1016/j.electacta.2019.135474>

107. Antolini E (2009) Carbon supports for low-temperature fuel cell catalysts. *Appl Catal B-Environ* 88: 1–24. <https://doi.org/10.1016/j.apcatb.2008.09.030>

108. Chen G, Dodson B, Hedges DM, et al. (2018) Fabrication of high aspect ratio millimeter-tall free-standing carbon nanotube-based microelectrode arrays. *ACS Biomater Sci Eng* 4: 1900–1907. <https://doi.org/10.1021/acsbiomaterials.8b00038>

109. Tian Z, Jiang S, Liang Y, et al. (2006) Synthesis and characterization of platinum catalysts on multiwalled carbon nanotubes by intermittent microwave irradiation for fuel cell applications. *J Phys Chem B* 110: 5343–5350. <https://doi.org/10.1021/jp056401o>

110. Hsieh C, Chou Y, Lin J (2007) Fabrication and electrochemical activity of Ni-attached carbon nanotube electrodes for hydrogen storage in alkali electrolyte. *Int J Hydrogen Energy* 32: 3457–3464. <https://doi.org/10.1016/j.ijhydene.2007.02.021>

111. Tang Z, Poh C, Lee K, et al. (2010) Enhanced catalytic properties from platinum nanodots covered carbon nanotubes for proton-exchange membrane fuel cells. *J Power Sources* 195: 155–159. <https://doi.org/10.1016/j.jpowsour.2009.06.105>

112. Jha N, Ramesh P, Bekyarova E, et al. (2013) Functionalized single-walled carbon nanotube-based fuel cell benchmarked against US DOE 2017 technical targets. *Sci Rep* 3: 2257. <https://doi.org/10.1038/srep02257>

113. Lin J, Adame A, Kannan A (2010) Development of durable platinum nanocatalyst on carbon nanotubes for proton exchange membrane fuel cells. *J Electrochem Soc* 157: B846. <https://doi.org/10.1149/1.3367753>

114. Tian Z, Lim S, Poh C, et al. (2011) A highly order-structured membrane electrode assembly with vertically aligned carbon nanotubes for ultra-low Pt loading PEM fuel cells. *Adv Energy Mater* 1: 1205–1214. <https://doi.org/10.1002/aenm.201100371>

115. Zhang W, Minett A, Gao M, et al. (2011) Integrated high-efficiency Pt/carbon nanotube arrays for PEM fuel cells. *Adv Energy Mater* 1: 671–677. <https://doi.org/10.1002/aenm.201100092>

116. Guo D, Li H (2004) High dispersion and electrocatalytic properties of Pt nanoparticles on SWNT bundles. *J Electroanal Chem* 573: 197–202. <https://doi.org/10.1016/j.jelechem.2004.07.006>

117. Shen A, Zou Y, Wang Q, et al. (2014) Oxygen reduction reaction in a droplet on graphite: Direct evidence that the edge is more active than the basal plane. *Angew Chem Int Ed* 53: 10804–10808. <https://doi.org/10.1002/ange.201406695>

118. Wang X, Wang J, Wang D, et al. (2014) One-pot synthesis of nitrogen and sulfur co-doped graphene as efficient metal-free electrocatalysts for the oxygen reduction reaction. *Chem Commun* 50: 4839–4842. <https://doi.org/10.1039/C4CC00440J>

119. Li T, Luo G, Liu K, et al. (2018) Encapsulation of Ni<sub>3</sub>Fe nanoparticles in N-doped carbon nanotube-grafted carbon nanofibers as high-efficiency hydrogen evolution electrocatalysts. *Adv Funct Mater* 28: 1805828. <https://doi.org/10.1002/adfm.201805828>

120. Sawant S, Patwardhan A, Joshi J, et al. (2022) Boron doped carbon nanotubes: Synthesis, characterization and emerging applications—A review. *Chem Eng J* 427: 131616. <https://doi.org/10.1016/j.cej.2021.131616>

121. Jarrais B, Guedes A, Freire C (2018) Heteroatom-doped carbon nanomaterials as metal-free catalysts for the reduction of 4-nitrophenol. *ChemistrySelect* 3: 1737–1748. <https://doi.org/10.1002/slct.201702706>

122. Akula S, Parthiban V, Peera S, et al. (2017) Simultaneous Co-doping of nitrogen and fluorine into MWCNTs: An in-situ conversion to graphene like sheets and its electro-catalytic activity toward oxygen reduction reaction. *J Electrochem Soc* 164: F568. <https://doi.org/10.1149/2.0501706jes>

123. Peera S, Menon R, Das S, et al. (2024) Oxygen reduction electrochemistry at F doped carbons: A review on the effect of highly polarized CF bonding in catalysis and stability of fuel cell catalysts. *Coordin Chem Rev* 500: 215491. <https://doi.org/10.1016/j.ccr.2023.215491>

124. Star AG, Fuller TF (2017) FIB-SEM tomography connects microstructure to corrosion-induced performance loss in PEMFC cathodes. *J Electrochem Soc* 164: F901. <https://doi.org/10.1149/2.0321709jes>

125. Park JH, Hwang SM, Park GG, et al. (2018) Variations in performance-degradation behavior of Pt/CNF and Pt/C MEAs for the same degree of carbon corrosion. *Electrochim Acta* 260: 674–683. <https://doi.org/10.1016/j.electacta.2017.12.015>

126. Kanninen P, Eriksson B, Davodi F, et al. (2020) Carbon corrosion properties and performance of multi-walled carbon nanotube support with and without nitrogen-functionalization in fuel cell electrodes. *Electrochim Acta* 332: 135384. <https://doi.org/10.1016/j.electacta.2019.135384>

127. Yu Y, Li H, Wang H, et al. (2012) A review on performance degradation of proton exchange membrane fuel cells during startup and shutdown processes: Causes, consequences, and mitigation strategies. *J Power Sources* 205: 10–23. <https://doi.org/10.1016/j.jpowsour.2012.01.059>

128. Earp B, Dunn D, Phillips J, et al. (2020) Enhancement of electrical conductivity of carbon nanotube sheets through copper addition using reduction expansion synthesis. *Mater Res Bull* 131: 110969. <https://doi.org/10.1016/j.materresbull.2020.110969>

129. Karthikeyan N, Vinayan B, Rajesh M, et al. (2015) Highly durable platinum based cathode electrocatalysts for PEMFC application using oxygen and nitrogen functional groups attached nanocarbon supports. *Fuel Cells* 15: 278–287. <https://doi.org/10.1002/fuce.201400134>

130. Zhao X, Hayashi A, Noda Z, et al. (2013) Evaluation of change in nanostructure through the heat treatment of carbon materials and their durability for the start/stop operation of polymer electrolyte fuel cells. *Electrochim Acta* 97: 33–41. <https://doi.org/10.1016/j.electacta.2013.02.062>

131. Wang M, Xu F, Sun H, et al. (2011) Nanoscale graphite-supported Pt catalysts for oxygen reduction reactions in fuel cells. *Electrochim Acta* 56: 2566–2573. <https://doi.org/10.1016/j.electacta.2010.11.019>

132. Wang X, Li W, Chen Z, et al. (2006) Durability investigation of carbon nanotube as catalyst support for proton exchange membrane fuel cell. *J Power Sources* 158: 154–159. <https://doi.org/10.1016/j.jpowsour.2005.09.039>

133. Gao W, Wen D, Ho J, et al. (2019) Incorporation of rare earth elements with transition metal-based materials for electrocatalysis: a review for recent progress. *Mater Today Chem* 12: 266–281. <https://doi.org/10.1016/j.mtchem.2019.02.002>

134. Arumugam B, Kakade B, Tamaki T, et al. (2014) Enhanced activity and durability for the electroreduction of oxygen at a chemically ordered intermetallic PtFeCo catalyst. *RSC Adv* 4: 27510–27517. <https://doi.org/10.1039/C4RA04744C>

135. Peera SG, Lee TG, Sahu AK (2019) Pt-rare earth metal alloy/metal oxide catalysts for oxygen reduction and alcohol oxidation reactions: An overview. *Sustain Energ Fuels* 3: 1866–1891. <https://doi.org/10.1039/C9SE00082H>

136. Borghei M, Scotti G, Kanninen P, et al. (2014) Enhanced performance of a silicon microfabricated direct methanol fuel cell with PtRu catalysts supported on few-walled carbon nanotubes. *Energy* 65: 612–620. <https://doi.org/10.1016/j.energy.2013.11.067>

137. López-Rosas D, Félix-Navarro R, Flores-Hernández J, et al. (2021) Synthesis of Pt-Ni/CNT cathodic catalyst and its application in a PEM fuel cell. *J Mex Chem Soc* 65: 39–51. <https://doi.org/10.29356/jmcs.v65i1.1268>

138. Wang H, Kakade BA, Tamaki T, et al. (2014) Synthesis of 3D graphite oxide-exfoliated carbon nanotube carbon composite and its application as catalyst support for fuel cells. *J Power Sources* 260: 338–348. <https://doi.org/10.1016/j.jpowsour.2014.03.014>

139. Garapati MS, Sundara R (2019) Highly efficient and ORR active platinum-scandium alloy-partially exfoliated carbon nanotubes electrocatalyst for proton exchange membrane fuel cell. *Int J Hydrogen Energy* 44: 10951–10963. <https://doi.org/10.1016/j.ijhydene.2019.02.161>

140. He Z, Chen J, Liu D, et al. (2004) Electrodeposition of Pt–Ru nanoparticles on carbon nanotubes and their electrocatalytic properties for methanol electrooxidation. *Diam Relat Mater* 13: 1764–1770. <https://doi.org/10.1016/j.diamond.2004.03.004>

141. Sharifi T, Nitze F, Barzegar HR, et al. (2012) Nitrogen doped multi walled carbon nanotubes produced by CVD-correlating XPS and Raman spectroscopy for the study of nitrogen inclusion. *Carbon* 50: 3535–3541. <https://doi.org/10.1016/j.carbon.2012.03.022>

142. Mardle P, Ji X, Wu J, et al. (2020) Thin film electrodes from Pt nanorods supported on aligned N-CNTs for proton exchange membrane fuel cells. *Appl Catal B-Environ* 260: 118031. <https://doi.org/10.1016/j.apcatb.2019.118031>

143. Liu Z, Shi Q, Zhang R, et al. (2014) Phosphorus-doped carbon nanotubes supported low Pt loading catalyst for the oxygen reduction reaction in acidic fuel cells. *J Power Sources* 268: 171–175. <https://doi.org/10.1016/j.jpowsour.2014.06.036>

144. Hoque M, Hassan F, Jauhar A, et al. (2018) Web-like 3D architecture of Pt nanowires and sulfur-doped carbon nanotube with superior electrocatalytic performance. *ACS Sustainable Chem Eng* 6: 93–98. <https://doi.org/10.1021/acssuschemeng.7b03580>

145. Rowshanzamir S, Peighambardoust SJ, Parnian M, et al. (2015) Effect of Pt-Cs<sub>2.5</sub>H<sub>0.5</sub>PW<sub>12</sub>O<sub>40</sub> catalyst addition on durability of self-humidifying nanocomposite membranes based on sulfonated poly(ether ether ketone) for proton exchange membrane fuel cell applications. *Int J Hydrogen Energy* 40: 549–560. <https://doi.org/10.1016/j.ijhydene.2014.10.134>

146. Shi X, Iqbal N, Kunwar S, et al. (2018) PtCo@NCNTs cathode catalyst using ZIF-67 for proton exchange membrane fuel cell. *Int J Hydrogen Energy* 43: 3520–3526. <https://doi.org/10.1016/j.ijhydene.2017.06.084>

147. Roudbari M, Ojani R, Raoof JB (2020) Nitrogen functionalized carbon nanotubes as a support of platinum electrocatalysts for performance improvement of ORR using fuel cell cathodic half-cell. *Renewable Energ* 159: 1015–1028. <https://doi.org/10.1016/j.renene.2020.06.028>

148. Ortiz-Herrera J, Cruz-Martínez H, Solorza-Feria O, et al. (2022) Recent progress in carbon nanotubes support materials for Pt-based cathode catalysts in PEM fuel cells. *Int J Hydrogen Energy* 47: 30213–30224. <https://doi.org/10.1016/j.ijhydene.2022.03.218>

149. Zhao T, Gadipelli S, He G, et al. (2018) Tunable bifunctional activity of Mn<sub>x</sub>Co<sub>3-x</sub>O<sub>4</sub> nanocrystals decorated on carbon nanotubes for oxygen electrocatalysis. *ChemSusChem* 11: 1295–1304. <https://doi.org/10.1002/cssc.201800049>

150. Ge X, Liu Y, Goh FT, et al. (2014) Dual-phase spinel MnCo<sub>2</sub>O<sub>4</sub> and spinel MnCo<sub>2</sub>O<sub>4</sub>/nanocarbon hybrids for electrocatalytic oxygen reduction and evolution. *ACS Appl Mater Interfaces* 6: 12684–12691. <https://doi.org/10.1021/am502675c>

151. Xing X, Liu R, Anjass M, et al. (2020) Bimetallic manganese-vanadium functionalized N,S-doped carbon nanotubes as efficient oxygen evolution and oxygen reduction electrocatalysts. *Appl Catal B-Environ* 277: 119195. <https://doi.org/10.1016/j.apcatb.2020.119195>

152. Li J, Tang D, Hou P, et al. (2018) The effect of carbon support on the oxygen reduction activity and durability of single-atom iron catalysts. *MRS Commun* 8: 1158–1166. <https://doi.org/10.1557/mrc.2018.174>

153. Esfahani R, Fruehwald H, Afsahi F, et al. (2018) Enhancing fuel cell catalyst layer stability using a dual-function sulfonated silica-based ionomer. *Appl Catal B-Environ* 232: 314–321. <https://doi.org/10.1016/j.apcatb.2018.03.080>

154. Moghadam Esfahani R, Vankova S, Easton E, et al. (2020) A hybrid Pt/NbO/CNTs catalyst with high activity and durability for oxygen reduction reaction in PEMFC. *Renew Energ* 154: 913–924. <https://doi.org/10.1016/j.renene.2020.03.029>

155. Liu Q, Li X, Zhang S, et al. (2022) Novel sulfonated N-heterocyclic poly(aryl ether ketone ketone)s with pendant phenyl groups for proton exchange membrane performing enhanced oxidative stability and excellent fuel cell properties. *J Membrane Sci* 641: 119926. <https://doi.org/10.1016/j.memsci.2021.119926>

156. Pan M, Pan C, Li C, et al. (2021) A review of membranes in proton exchange membrane fuel cells: Transport phenomena, performance and durability. *Renew Sust Energ Rev* 141: 110771. <https://doi.org/10.1016/j.rser.2021.110771>

157. Sun X, Simonsen SC, Norby T, et al. (2019) Composite membranes for high temperature PEM fuel cells and electrolyzers: A critical review. *Membranes* 9: 83. <https://doi.org/10.3390/membranes9070083>

158. Chen J, Liu B, Gao X, et al. (2018) A review of the interfacial characteristics of polymer nanocomposites containing carbon nanotubes. *RSC Adv* 8: 28048–28085. <https://doi.org/10.1039/C8RA04205E>

159. Taufiq M, Shaari N, Kamarudin S (2021) Carbon nanotube, graphene oxide and montmorillonite as conductive fillers in polymer electrolyte membrane for fuel cell: an overview. *Int J Energy Res* 45: 1309–1346. <https://doi.org/10.1002/er.5874>

160. Asgari M, Nikazar M, Molla-Abbas P, et al. (2013) Nafion®/histidine functionalized carbon nanotube: High-performance fuel cell membranes. *Int J Hydrogen Energy* 38: 5894–5902. <https://doi.org/10.1016/j.ijhydene.2013.03.010>

161. Steffy N, Parthiban V, Sahu A (2018) Uncovering Nafion-multiwalled carbon nanotube hybrid membrane for prospective polymer electrolyte membrane fuel cell under low humidity. *J Membrane Sci* 563: 65–74. <https://doi.org/10.1016/j.memsci.2018.05.051>

162. Kim A, Gabunada J, Yoo D (2019) Amelioration in physicochemical properties and single cell performance of sulfonated poly (ether ether ketone) block copolymer composite membrane using sulfonated carbon nanotubes for intermediate humidity fuel cells. *Int J Energy Res* 43: 2974–2989. <https://doi.org/10.1002/er.4494>

163. Neelakandan S, Kanagaraj P, Sabarathinam R, et al. (2016) Effect of sulfonated graphene oxide on the performance enhancement of acid–base composite membranes for direct methanol fuel cells. *RSC Adv* 6: 51599–51608. <https://doi.org/10.1039/C5RA27655A>

164. Ahmed S, Ali M, Cai Y, et al. (2019) Novel sulfonated multi-walled carbon nanotubes filled chitosan composite membrane for fuel-cell applications. *J Appl Polym Sci* 136: 47603. <https://doi.org/10.1002/app.47603>

165. Matos B, Santiago E, Fonseca F, et al. (2007) Nafion–titanate nanotube composite membranes for PEMFC operating at high temperature. *J Electrochem Soc* 154: B1358. <https://doi.org/10.1149/1.2790802>

166. Gentil S, Lalaoui N, Dutta A, et al. (2017) Carbon-nanotube-supported bio-inspired nickel catalyst and its integration in hybrid hydrogen/air fuel cells. *Angew Chem Int Ed* 129: 1871–1875. <https://doi.org/10.1002/ange.201611532>

167. Yi P, Zhang D, Qiu D, et al. (2019) Carbon-based coatings for metallic bipolar plates used in proton exchange membrane fuel cells. *Int J Hydrogen Energy* 44: 6813–6843. <https://doi.org/10.1016/j.ijhydene.2019.01.176>

168. Hu Q, Zhang D, Fu H (2015) Effect of flow-field dimensions on the formability of Fe–Ni–Cr alloy as bipolar plate for PEM (proton exchange membrane) fuel cell. *Energy* 83: 156–163. <https://doi.org/10.1016/j.energy.2015.02.010>

169. Papadias DD, Ahluwalia RK, Thomson JK, et al. (2015) Degradation of SS316L bipolar plates in simulated fuel cell environment: Corrosion rate, barrier film formation kinetics and contact resistance. *J Power Sources* 273: 1237–1249. <https://doi.org/10.1016/j.jpowsour.2014.02.053>

170. Daricik F, Topcu A, Aydin K, et al. (2023) Carbon nanotube (CNT) modified carbon fiber/epoxy composite plates for the PEM fuel cell bipolar plate application. *Int J Hydrogen Energy* 48: 1090–1106. <https://doi.org/10.1016/j.ijhydene.2022.09.297>

171. Ramírez-Herrera C, Tellez-Cruz M, Pérez-González J, et al. (2021) Enhanced mechanical properties and corrosion behavior of polypropylene/multi-walled carbon nanotubes/carbon nanofibers nanocomposites for application in bipolar plates of proton exchange membrane fuel cells. *Int J Hydrogen Energy* 46: 26110–26125. <https://doi.org/10.1016/j.ijhydene.2021.04.125>

172. Radzuan N, Sulong A, Somalu M, et al. (2019) Fibre orientation effect on polypropylene/milled carbon fiber composites in the presence of carbon nanotubes or graphene as a secondary filler: Application on PEM fuel cell bipolar plate. *Int J Hydrogen Energy* 44: 30618–30626. <https://doi.org/10.1016/j.ijhydene.2019.01.063>

173. Dhakate S, Sharma S, Chauhan N, et al. (2010) CNTs nanostructuring effect on the properties of graphite composite bipolar plate. *Int J Hydrogen Energy* 35: 4195–4200. <https://doi.org/10.1016/j.ijhydene.2010.02.072>

174. Witpathomwong S, Okhawilai M, Jubsilp C, et al. (2020) Highly filled graphite/graphene/carbon nanotube in polybenzoxazine composites for bipolar plate in PEMFC. *Int J Hydrogen Energy* 45: 30898–30910. <https://doi.org/10.1016/j.ijhydene.2020.08.006>

175. Bairan A, Selamat MZ, Sahadan SN, et al. (2016) Effect of carbon nanotubes loading in multifiller polymer composite as bipolar plate for PEM fuel cell. *Procedia Chem* 19: 91–97. <https://doi.org/10.1016/j.proche.2016.03.120>

176. Suherman H, Sulong AB, Sahari J (2013) Effect of the compression molding parameters on the in-plane and through-plane conductivity of carbon nanotubes/graphite/epoxy nanocomposites as bipolar plate material for a polymer electrolyte membrane fuel cell. *Ceram Int* 39: 1277–1284. <https://doi.org/10.1016/j.ceramint.2012.07.059>

177. Selamat MZ, Ahmad MS, bin Daud MA, et al. (2013) Effect of carbon nanotubes on properties of graphite/carbon black/polypropylene nanocomposites. *Adv Mat Res* 795: 29–34. <https://doi.org/10.4028/www.scientific.net/AMR.795.29>

178. Hu B, Chang FL, Xiang LY, et al. (2021) High performance polyvinylidene fluoride/graphite/multi-walled carbon nanotubes composite bipolar plate for PEMFC with segregated conductive networks. *Int J Hydrogen Energy* 46: 25666–25676. <https://doi.org/10.1016/j.ijhydene.2021.05.081>

179. de Oliveira M, Ett G, Antunes RA (2013) Corrosion and thermal stability of multi-walled carbon nanotube–graphite–acrylonitrile–butadiene–styrene composite bipolar plates for polymer electrolyte membrane fuel cells. *J Power Sources* 221: 345–355. <https://doi.org/10.1016/j.jpowsour.2012.08.052>

180. Show Y, Takahashi K (2009) Stainless steel bipolar plate coated with carbon nanotube (CNT)/polytetrafluoroethylene (PTFE) composite film for proton exchange membrane fuel cell (PEMFC). *J Power Sources* 190: 322–325. <https://doi.org/10.1016/j.jpowsour.2009.01.027>

181. Deyab M (2014) Corrosion protection of aluminum bipolar plates with polyaniline coating containing carbon nanotubes in acidic medium inside the polymer electrolyte membrane fuel cell. *J Power Sources* 268: 50–55. <https://doi.org/10.1016/j.jpowsour.2014.06.021>

182. Younas T (2022) Bipolar plates for the permeable exchange membrane: carbon nanotubes as an alternative, In: Kaur G, *PEM Fuel Cells*, Amsterdam: Elsevier. <https://doi.org/10.1016/B978-0-12-823708-3.00004-3>

183. Yao K, Adams D, Hao A, et al. (2017) Highly conductive and strong graphite-phenolic resin composite for bipolar plate applications. *Energy Fuels* 31: 14320–14331. <https://doi.org/10.1021/acs.energyfuels.7b02678>

184. Kwon O, Kim J, Choi H, et al. (2022) CNT sheet as a cathodic functional interlayer in polymer electrolyte membrane fuel cells. *Energy* 245: 123237. <https://doi.org/10.1016/j.energy.2022.123237>

185. Makharia R, Mathias MF, Baker DR (2005) Measurement of catalyst layer electrolyte resistance in PEFCs using electrochemical impedance spectroscopy. *J Electrochem Soc* 152: A970. <https://doi.org/10.1149/1.1888367>

186. Kim J, Kim H, Song H, et al. (2021) Carbon nanotube sheet as a microporous layer for proton exchange membrane fuel cells. *Energy* 227: 120459. <https://doi.org/10.1016/j.energy.2021.120459>

187. Holzapfel P, Bühler M, Escalera-López D, et al. (2020) Fabrication of a robust PEM water electrolyzer based on non-noble metal cathode catalyst:  $[Mo_3S_13]^{2-}$  clusters anchored to N-doped carbon nanotubes. *Small* 16: 2003161. <https://doi.org/10.1002/smll.202003161>

188. Sonawane J, Yadav A, Ghosh P, et al. (2017) Recent advances in the development and utilization of modern anode materials for high performance microbial fuel cells. *Biosens Bioelectron* 90: 558–576. <https://doi.org/10.1016/j.bios.2016.10.014>

189. Rikame SS, Mungray AA, Mungray AK (2018) Modification of anode electrode in microbial fuel cell for electrochemical recovery of energy and copper metal. *Electrochim Acta* 275: 8–17. <https://doi.org/10.1016/j.electacta.2018.04.141>

190. Wang Y, Cheng X, Liu K, et al. (2022) 3D hierarchical  $Co_8FeS_8$ - $FeCO_2O_4$ /N-CNTs@CF with an enhanced microorganisms–anode interface for improving microbial fuel cell performance. *ACS Appl Mater Interfaces* 14: 35809–35821. <https://doi.org/10.1021/acsami.2c09622>

191. Zhao N, Ma Z, Song H, et al. (2019) Enhancement of bioelectricity generation by synergistic modification of vertical carbon nanotubes/polypyrrole for the carbon fibers anode in microbial fuel cell. *Electrochim Acta* 296: 69–74. <https://doi.org/10.1016/j.electacta.2018.11.039>

192. Wu X, Qiao Y, Guo C, et al. (2020) Nitrogen doping to atomically match reaction sites in microbial fuel cells. *Commun Chem* 3: 68. <https://doi.org/10.1038/s42004-020-0316-z>

193. Iftimie S, Dumitru A (2019) Enhancing the performance of microbial fuel cells (MFCs) with nitrophenyl modified carbon nanotubes-based anodes. *Appl Surf Sci* 492: 661–668. <https://doi.org/10.1016/j.apsusc.2019.06.241>

194. Ren H, Pyo S, Lee JI, et al. (2015) A high power density miniaturized microbial fuel cell having carbon nanotube anodes. *J Power Sources* 273: 823–830. <https://doi.org/10.1016/j.jpowsour.2014.09.165>

195. Dumitru A, Vulpe S, Radu A, et al. (2018) Influence of nitrogen environment on the performance of conducting polymers/CNTs nanocomposites modified anodes for microbial fuel cells (MFCs). *Rom J Phys* 63: 605–625. Available from: [https://rjp.nipne.ro/2018\\_63\\_3-4/RomJPhys.63.605.pdf](https://rjp.nipne.ro/2018_63_3-4/RomJPhys.63.605.pdf).

196. Mehdinia A, Ziae E, Jabbari A (2014) Multi-walled carbon nanotube/SnO<sub>2</sub> nanocomposite: A novel anode material for microbial fuel cells. *Electrochim Acta* 130: 512–518. <https://doi.org/10.1016/j.electacta.2014.03.011>

197. Fu Y, Yu J, Zhang Y, et al. (2014) Graphite coated with manganese oxide/multiwall carbon nanotubes composites as anodes in marine benthic microbial fuel cells. *Appl Surf Sci* 317: 84–89. <https://doi.org/10.1016/j.apsusc.2014.08.044>

198. Wen Z, Ci S, Mao S, et al. (2013) TiO<sub>2</sub> nanoparticles-decorated carbon nanotubes for significantly improved bioelectricity generation in microbial fuel cells. *J Power Sources* 234: 100–106. <https://doi.org/10.1016/j.jpowsour.2013.01.146>

199. Schulze M, Gülvaz E (2004) Degradation of nickel anodes in alkaline fuel cells. *J Power Sources* 127: 252–263. <https://doi.org/10.1016/j.jpowsour.2003.09.021>

200. Liu Y, Shao Z, Mori T (2021) Development of nickel based cermet anode materials in solid oxide fuel cells—Now and future. *Mater Rep Energy* 1: 100003. <https://doi.org/10.1016/j.matre.2020.11.002>

201. Mink J, Rojas J, Logan B, et al. (2012) Vertically grown multiwalled carbon nanotube anode and nickel silicide integrated high performance microsized (1.25 μL) microbial fuel cell. *Nano Lett* 12: 791–795. <https://doi.org/10.1021/nl203801h>

202. Zhang H, Wang Y, Wu Z, et al. (2017) A direct urea microfluidic fuel cell with flow-through Ni-supported-carbon-nanotube-coated sponge as porous electrode. *J Power Sources* 363: 61–69. <https://doi.org/10.1016/j.jpowsour.2017.07.055>

203. Tesfaye R, Das G, Park B, et al. (2019) Ni-Co bimetal decorated carbon nanotube aerogel as an efficient anode catalyst in urea fuel cells. *Sci Rep* 9: 479. <https://doi.org/10.1038/s41598-018-37011-w>

204. Gonzalez-Reyna M, Luna-Martínez M, Perez-Robles J (2020) Nickel supported on carbon nanotubes and carbon nanospheres for ammonia oxidation reaction. *Nanotechnology* 31: 235706. <https://doi.org/10.1088/1361-6528/ab73b6>

205. Abrari S, Daneshvari-Esfahlan V, Hosseini M, et al. (2022) Multi-walled carbon nanotube-supported Ni@Pd core–shell electrocatalyst for direct formate fuel cells. *J Appl Electrochem* 52: 755–764. <https://doi.org/10.1007/s10800-022-01668-z>

206. Nourbakhsh F, Mohsennia M, Pazouki M (2017) Nickel oxide/carbon nanotube/polyaniline nanocomposite as bifunctional anode catalyst for high-performance *Shewanella*-based dual-chamber microbial fuel cell. *Bioproc Biosyst Eng* 40: 1669–1677. <https://doi.org/10.1007/s00449-017-1822-y>

207. Nazal M, Olakunle O, Al-Ahmed A, et al. (2018) Precious metal free Ni/Cu/Mo trimetallic nanocomposite supported on multi-walled carbon nanotubes as highly efficient and durable anode-catalyst for alkaline direct methanol fuel cells. *J Electroanal Chem* 823: 98–105. <https://doi.org/10.1016/j.jelechem.2018.05.035>

208. Liu Y, Zhou G, Sun Y, et al. (2023) Hollow cobalt ferrite nanofibers integrating with carbon nanotubes as microbial fuel cell anode for boosting extracellular electron transfer. *Appl Surf Sci* 609: 155386. <https://doi.org/10.1016/j.apsusc.2022.155386>

209. Fraiwan A, Adusumilli S, Han D, et al. (2014) Microbial power-generating capabilities on micro-/nano-structured anodes in micro-sized microbial fuel cells. *Fuel Cells* 14: 801–809. <https://doi.org/10.1002/fuce.201400041>

210. Cui H, Du L, Guo P, et al. (2015) Controlled modification of carbon nanotubes and polyaniline on macroporous graphite felt for high-performance microbial fuel cell anode. *J Power Sources* 283: 46–53. <https://doi.org/10.1016/j.jpowsour.2015.02.088>

211. Wang YQ, Huang HX, Li B, et al. (2015) Novelly developed three-dimensional carbon scaffold anodes from polyacrylonitrile for microbial fuel cells. *J Mater Chem A* 3: 5110–5118. <https://doi.org/10.1039/C4TA06007E>

212. Li J, Qian J, Chen X, et al. (2022) Three-dimensional hierarchical graphitic carbon encapsulated CoNi alloy/N-doped CNTs/carbon nanofibers as an efficient multifunctional electrocatalyst for high-performance microbial fuel cells. *Composites Part B* 231: 109573. <https://doi.org/10.1016/j.compositesb.2021.109573>

213. Yadav MD, Joshi HM, Sawant SV, et al. (2023) Advances in the application of carbon nanotubes as catalyst support for hydrogenation reactions. *Chem Eng Sci* 272: 118586. <https://doi.org/10.1016/j.ces.2023.118586>

214. Maturost S, Themsirimongkon S, Waenkaew P, et al. (2021) The effect of CuO on a Pt-based catalyst for oxidation in a low-temperature fuel cell. *Int J Hydrogen Energy* 46: 5999–6013. <https://doi.org/10.1016/j.ijhydene.2020.08.154>

215. Shrotri N, Daletou MK (2022) The Pt–Co alloying effect on the performance and stability of high temperature PEMFC cathodes. *Int J Hydrogen Energy* 47: 16235–16248. <https://doi.org/10.1016/j.ijhydene.2022.03.109>

216. Takenaka S, Goto M, Masuda Y, et al. (2018) Improvement in the durability of carbon black-supported Pt cathode catalysts by silica-coating for use in PEFCs. *Int J Hydrogen Energy* 43: 7473–7482. <https://doi.org/10.1016/j.ijhydene.2018.02.159>



AIMS Press

© 2024 the Author(s), licensee AIMS Press. This is an open access article distributed under the terms of the Creative Commons Attribution License (<http://creativecommons.org/licenses/by/4.0>)